PERGAMON

Journal of Structural Geology 24 (2002) 1369–1387

JOURNAL OF STRUCTURAL GEOLOGY

www.elsevier.com/locate/jstrugeo

Four-dimensional analysis of the inversion of a half-graben to form the Whittier fold–fault system of the Los Angeles basin

Tom Bjorklund, Kevin Burke

Department of Geosciences, University of Houston, 312 Science & Research Building 1, Houston, TX 77204-5007, USA

Received 28 March 2001; revised 15 August 2001; accepted 20 August 2001

Abstract

Analysis of structural and stratigraphic data from hundreds of oil wells, surface geologic maps and earthquake focal mechanisms reveals a three-phase structural evolution of the Whittier fold–fault system. That evolution progressed from an extensional phase (16 Ma), accommodated by the formation of a half-graben, through an episode of graben filling (14–8 Ma) to lithospheric shortening, which began (ca. 8 Ma) with contractional reactivation of the graben-forming fault as a blind reverse fault and accompanying anticlinal uplift. About 1 Ma, the blind reverse fault broke through onto the sea floor, initiating the activity of the present Whittier fault system. Horizontal contraction estimated from reconstructed cross-sections ranges from 1.4 to 3.2 km and has been at an average rate of 0.3 mm/year in the P direction (N–S) of the 1987 Whittier Narrows earthquake for the past ca. 8 My. That rate may have accelerated after breakthrough of the blind reverse fault to as much as 1.0 mm/year. The ratio of strike-slip to dip-slip displacement on the Whittier fault over the past ca. 8 My is about 0.4.

Keywords: Displacement; Half-graben; Puente Formation; Reverse fault; Whittier fault

1. Introduction

The tectonic evolution of the west coast of the United States has been dominated, since the beginning of the Neogene (ca. 24 Ma), by the change from a convergent to a transform margin that has accompanied the demise of the Farallon plate (Atwater, 1970). The complex operation of this process in southern California, including the formation and subsequent deformation of the Los Angeles basin, has received much attention during the past decade. Luyendyk (1991) and Nicholson et al. (1994) recognized the importance of a ca. 90° rotation of the Transverse Ranges between 18 and 5 Ma. Crouch and Suppe (1993) developed an analysis of lithospheric extension in the basin involving high-angle normal faults above a major detachment surface. Recent refinements include the suggestion that the Los Angeles basin experienced rapid subsidence after trans-rotational detachment faulting ended at 12 Ma and before the southern San Andreas fault became active in the area, at ca. 5 Ma (Nicholson et al., 1994; Ingersoll and Rumelhart, 1999). Later studies in the Gulf of California indicate that the present San Andreas fault may have become active in that area as early as ca. 6 Ma (Oskin et al., 2000) or even ca. 8 Ma (Axen, 2000). The regional tectonic importance of the interval between 8 and 5 Ma has been emphasized by the recognition of major elevation at the junction of the Peninsular and the Transverse Ranges at ca. 5 Ma (Wolf et al., 1997).

In this paper we analyze the Whittier fault (Fig. 1) as part of a fold–fault system that has evolved by inversion of a half-graben in the northeastern corner of the Los Angeles basin. The Whittier fold–fault system provides an unusually complete record of the processes that have operated within the Los Angeles basin over the past ca. 16 My because the Whittier area has been elevated above sea level within the past 1 My, exposing sedimentary and igneous rocks that record much of the history of the basin. Complementary subsurface structural and stratigraphic data from the Whittier area comes from hundreds of oil and gas wells. Finally, active deformation in the Los Angeles basin area is being investigated by paleoseismic studies in trenches, by GPS networks, by SAR interferometry, and by seismic networks.

The Whittier data set embraces a volume of ca. 2000 km^3 (covering 700 km^2 to a depth of 3 km) and records all the processes of extension, deposition, folding, faulting, intrusion, extrusion, and erosion within a 16 My interval. This unusually complete record has enabled us to prepare a 4-D interpretation of the evolution of the structure of this area. Preparation of cross-sections has been based on the balancing techniques described by Erslev (1986), Narr and Suppe (1994), Mitra and Mount (1998) and Novoa et al.

E-mail address: tbjorklund@uh.edu (T. Bjorklund).

0191-8141/02/$ - see front matter
PII: S0191-8141(01)00147-X

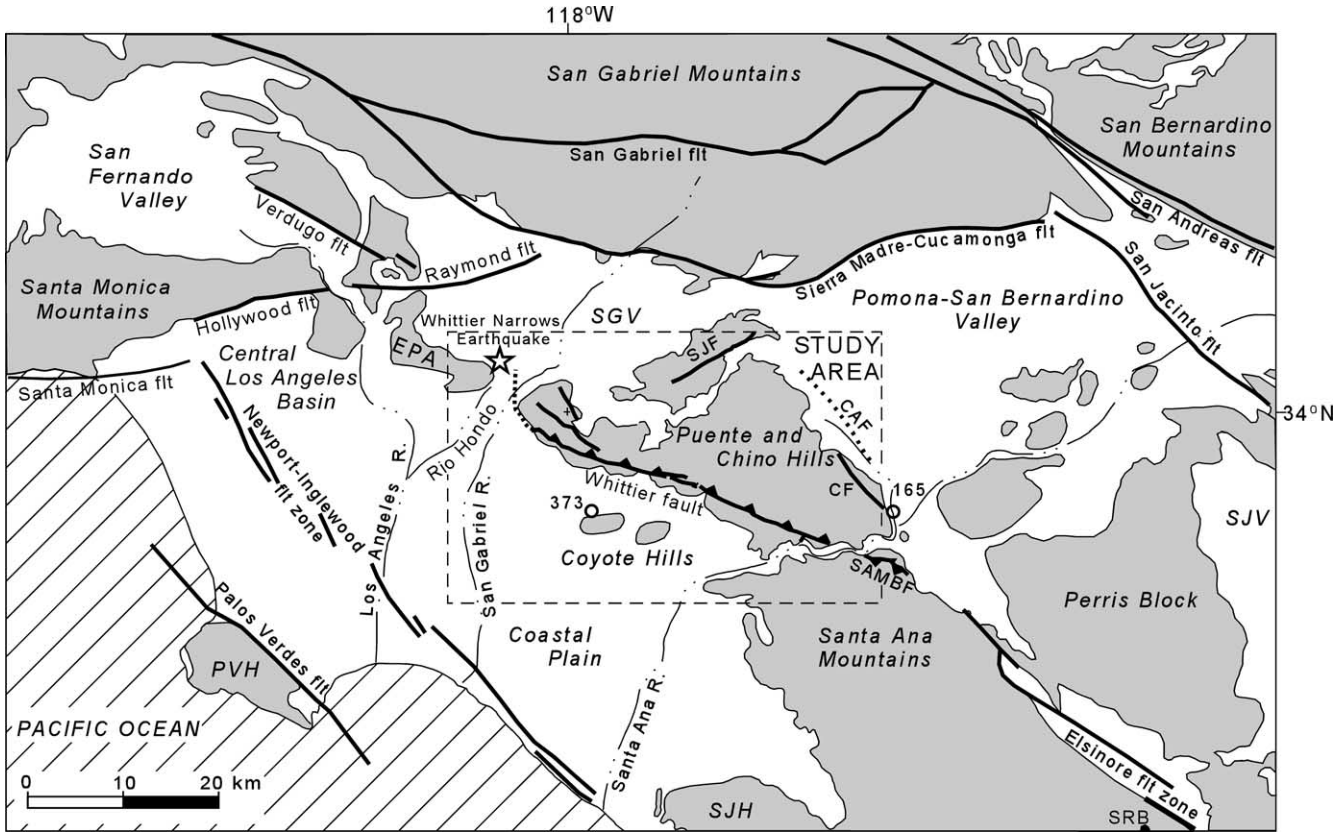

Fig. 1. Index map of the Los Angeles basin and surrounding uplifts. Dashed box is location of Figs. 3–5. Central Avenue fault (CAF), Chino fault (CF), Elysian Park Anticline (EPA), Palos Verdes Hills (PVH), San Gabriel Valley (SGV), San Jacinto Valley (SJV), San Jose Hills (SJH), Santa Rosa Basalt northernmost outcrop (SRB), Santa Ana Mountain Boundary Fault (SAMBF), Chevron Murphy–Coyote 373 (373), Prado Petroleum Government 165-1 (165).

(2000), and especially the procedure of Cook (1988) for structures associated with basement-involved faults (Appendix A). Interpretation of the Whittier structure in three dimensions has involved constructing a network of closely-spaced strike and dip cross-sections, which will be published in full elsewhere (Bjorklund, in preparation). Restoration of cross-sections through time has given a fourth dimension to our analysis. We suggest that this analysis of the Whittier fault, because of the wealth of surface and subsurface data used in the study, may prove to be a useful guide in helping to assess the strengths and the limitations of the methods used in preparing structural restorations where less complete data-sets are available. We hope that our work may be a useful guide not only in other parts of the Los Angeles basin but more generally in the analysis of structural inversion.

2. Stratigraphy and geologic history

2.1. Basement rocks: Bedford Canyon Formation, Santa Monica Formation, Santiago Peak Volcanics and Southern California batholith intrusions (160–90 Ma)

Rocks of an Andean-type arc-trench system of Mesozoic age (e.g. Barth and Schneiderman, 1996) form the basement of the area now occupied by the Whittier fold–fault system. The Bedford Canyon Formation accretionary-wedge complex forming the core of the Santa Ana Mountains is the oldest unit that crops out in the area (Fig. 2). Santiago Peak Volcanics (ca. 140 Ma) (Fife et al., 1967, Dickinson and Lawton, 2001) unconformably and discontinuously overlie the Bedford Canyon Formation (ca. 160 Ma) (Imlay, 1964), and magmatic-arc rocks of the Southern California batholith (ca. 95 Ma) (Banks and Silver, 1966) intrude both units (Schoellhamer et al., 1981).

2.2. Forearc sedimentary strata: Trabuco, Ladd, Williams, Silverado, Santiago and Sespe and Vaqueros Formations (90–16 Ma)

The Andean-type arc system of California, which persisted in some form until earliest Neogene time (ca. 24 Ma) in the Los Angeles basin area is represented in the Santa Ana Mountains by about 3500 m of forearc marine and non-marine sandstones and conglomerates and except for the Holz Shale Member, which forms the upper part of the Ladd Formation (Fig. 2), are mechanically competent (Schoellhamer et al., 1981; McCulloh et al., 2000). The less competent Holz unit possibly served to localize detachment

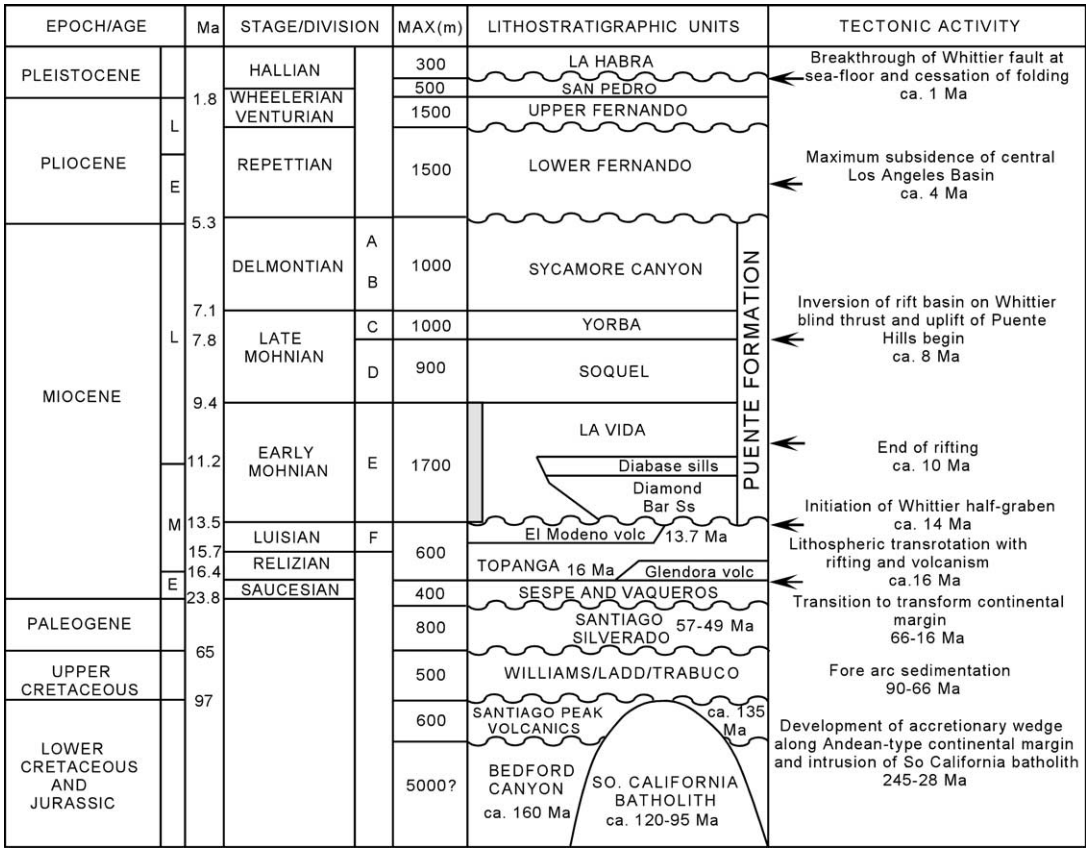

Fig. 2. Stratigraphic column. Shaded bar shows oil source rock interval. MAX (m) indicates approximate maximum thickness of a unit in meters in the study area. Cenozoic ages from Turner (1970), Blake (1991), Berggren et al. (1995), McCulloh et al. (2000) and Barron and Isaacs (2001). Mesozoic ages from Larsen et al. (1958), Imlay (1964), Banks and Silver (1966), Fife et al. (1967). Divisions A through F are benthic foraminiferal divisions from Wissler (1943) with ages of division boundaries from Blake (1991) and Barron and Isaacs (2001). Time of maximum subsidence of Los Angeles basin from Ingersoll and Rumelhart (1999, Fig. 3).

surfaces (West and Redin, 1991). Shallow-marine and coarse non-marine deposits of the Sespe and Vaqueros Formations characterize the final phase of the transition from the Andean-type continental margin to the Neogene transform-type margin (Nilsen, 1987).

2.3. Transform-margin strata (16–0 Ma)

Miocene and Pliocene strata of the Los Angeles transform-margin basin (post-Sespe and Vaqueros Formations) consist of a basal unit of shallow-water marine sandstone, overlying bathyal sandstone, siltstone and shale representing turbidites and biogenic sediments and minor amounts of igneous intrusive and extrusive rocks. Shallow-marine and non-marine Pleistocene silt, sand and gravel of the San Pedro and La Habra Formations crop out on the flanks of uplifts surrounding the Los Angeles coastal plain. The full Los Angeles basin section is over 6000 m thick in the southwestern part of our study area. The detailed lithologic characteristics of the Los Angeles basin section in the study area were described by Durham and Yerkes (1964), Yerkes (1972), Schoellhamer et al. (1981), Blake (1991) and Yeats and Beall (1991).

2.3.1. Strata of the extensional phase: Glendora Volcanics, Topanga Formation, La Vida and Soquel Members of the Puente Formation (16–7.8 Ma)

Middle Miocene Glendora Volcanics that underlie and are interbedded with the marine Topanga Formation (Fig. 2) record the onset of rifting in the northeastern Los Angeles basin (Hornafius et al., 1986; Mayer, 1991; Rumelhart and Ingersoll, 1997; Ingersoll and Rumelhart, 1999). The age of the Glendora Volcanics ranges from ca. 16 to 14 Ma (Blake, 1991; Nourse et al., 1998). The Topanga sandstone has been penetrated by drill holes over most of the study area and is thickest in wells north of the Brea–Olinda oil field, reaching an estimated thickness of 700 m (Aera Energy Puente A-3) (Fig. 3); it pinches out to the northwest. This mechanically competent sandstone and its associated volcanic rocks contrast with the mechanically incompetent, thinly-bedded shale and siltstone of the overlying Puente Formation, which in outcrop commonly display intense, small-scale disharmonic folding.

The La Vida Member, at the base of the Puente Formation, typically consists of thinly bedded siltstone with subordinate amounts of sandstone. In outcrops and wells in the Puente Hills, the lower part of the La Vida

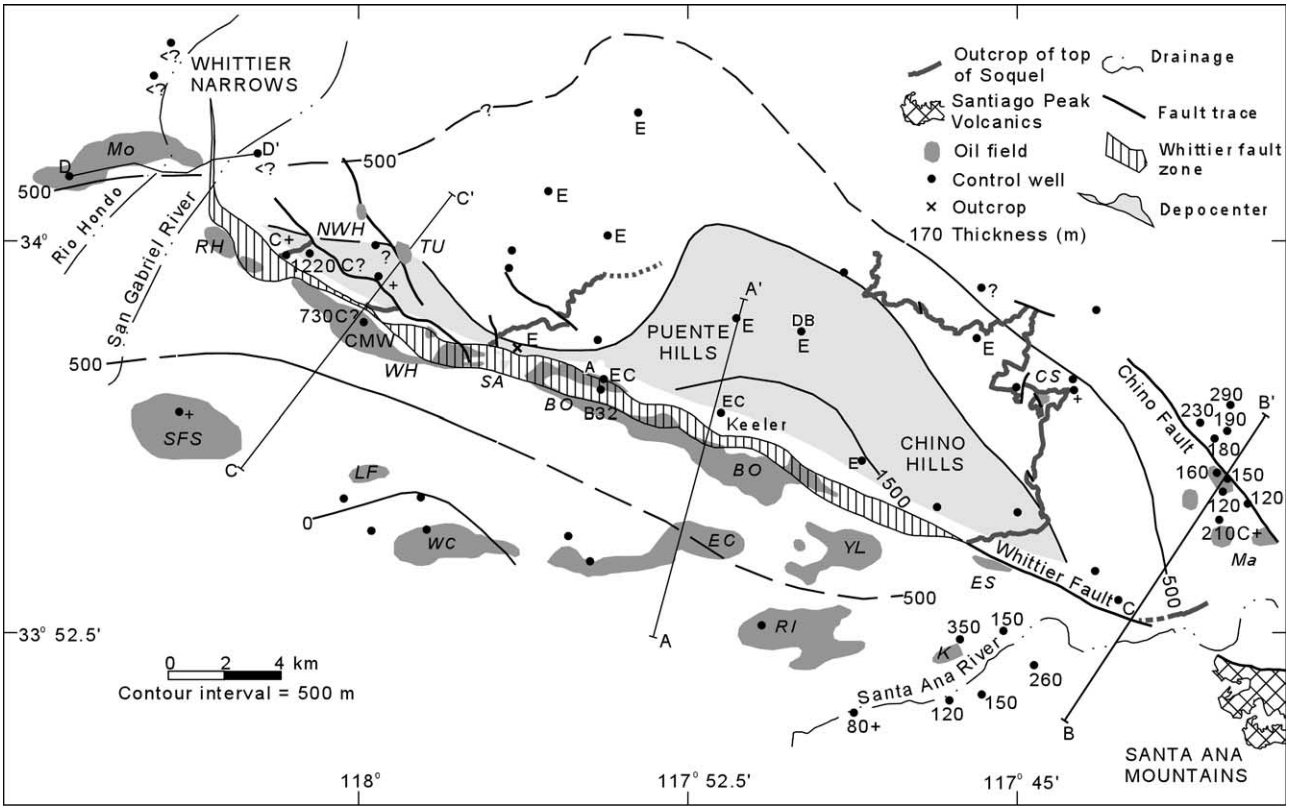

Fig. 3. Isopach map of the La Vida Member of the Puente Formation. Contours indicate approximate stratigraphic thickness. The thick section in the hanging wall block includes the siltstone, sandstone and diabase units that are only present north of the Whittier fault. The Whittier fault zone is the area of overlap between the footwall and hanging wall cutoffs of the top of the Soquel Member. Because the map is not a palinspastic map, contours do not cross the Whittier fault. Contours dashed where not well constrained and queried where speculative. Section missing by erosion estimated (E), thickness corrected for bed dip (C), incomplete penetration of unit by wellbore (+), correlation uncertainty (?), Puente Formation penetrated but La Vida Member contacts uncertain (<?), no annotation (wellbore thickness). Key wells are Aera Energy Puente A-3 (A3) and Puente B32 (B32), Chevron Murphy–Whittier 304 (304), Shell Keeler Community 1 (Keeler), Western Gulf Diamond Bar 1 (DB). Oil fields are Chino–Soquel (CS), Brea–Olinda (BO), East Coyote (EC), Esperanza (Es), Kraemer (K), Leffingwell (LF), Mahala (Ma), Montebello (Mo), North Whittier Heights (NWhH), Richfield (Ri), Rideout Heights (RH), Sansinena (Sa), Santa Fe Springs (SFS), Turnbull (Tu), West Coyote (WC), Whittier (Wh) and Yorba Linda (YL). Data from Yerkes (1972), Durham and Yerkes (1962), Schoellhamer et al. (1981), Yeats and Beall (1991) and West and Redin (1991).

Member contains extensive, stacked, diabase intrusions individually as thick as 200 m. Although speculatively correlated with the Santa Rosa Basalt (ca. 7–10.6 Ma) (Morton and Morton, 1979), located east of the Santa Ana Mountains (McCulloh et al., 2000), no definitive radiometic dates have been determined for the diabase. The diabase sills are younger than the enclosing lower La Vida siltstone (younger than 13.9 Ma) (Blake, 1991) and probably older than ca. 8 Ma (the beginning of the compressional phase recognized by this study.) The Diamond Bar sandstone, a well-cemented, conglomeratic unit penetrated in the Western Gulf Diamond Bar 1 well (Fig. 3) and named by Woodford et al. (1944), was placed in the Topanga sandstone by Durham and Yerkes, 1964), but we follow Yeats and Beall (1991, Fig. 2H and J) by including the Diamond Bar sandstone in the lower part of the La Vida Member. Inclusion of the Diamond Bar in the Topanga sandstone requires compensating thickening of the Topanga and thinning of the Diamond Bar that is not reasonable over the short distances involved and results in subsurface dips that are not consistent with surface data. The Diamond Bar sandstone contains volcanic debris from underlying rocks (Durham and Yerkes, 1964), which suggests that fossils of Luisian age reported to have been found in parts of the sandstone (Beyer, personal communication) could have been derived from the underlying rocks. Well correlations clearly establish the interbedded relationships among the Diamond Bar sandstone, the diabase sills and the La Vida siltstone. Neither the diabase nor the Diamond Bar sandstone is known south of the Whittier fault. Because of the presence of these units and associated siltstone interbeds north of the Whittier fault, the La Vida Member is thicker there than south of the fault. North of the fault, the isopach contours of the La Vida Member define a wedge-shaped body of rocks (Fig. 3).

The overlying Soquel Member of the Puente Formation is a widespread, conglomeratic sandstone interbedded with siltstone. In the subsurface at the Brea–Olinda oil field, close to the Whittier fault, the Soquel Member is locally mainly siltstone. The top of microfaunal Division D

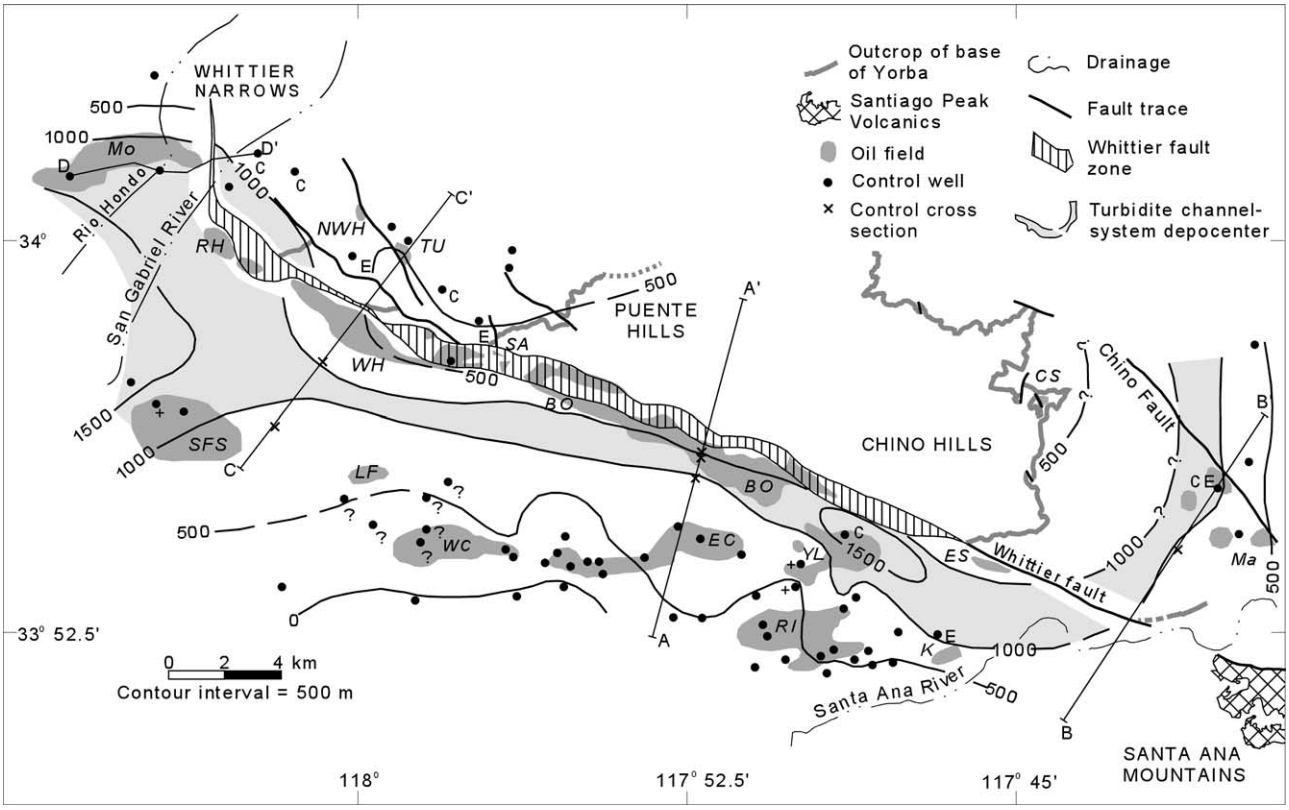

Fig. 4. Isopach map of Sycamore Canyon and Yorba Members of Puente Formation. The trend of the thickest part of the unit generally delineates the location of a turbidite fan-channel system (Redin, 1991). See Fig. 3 for explanation of symbols, references and names of oil fields.

(ca. 7.8 Ma) in the Brea–Olinda oil field is placed close to the top of the Soquel sandstone (Blake, 1991). Largely because of the approximate equivalence of these paleontologic and lithologic horizons, the Soquel Member has proven to be the only stratigraphic unit that we have been able to correlate in the subsurface and, by restoration of partly eroded sections, at the surface over most of our study area. The Soquel Member ranges in thickness up to nearly 900 m in Richfield oil field but generally ranges from 50 to 600 m in the study area.

2.3.2. Strata of the contractional phase: Yorba and Sycamore Canyon Members of the Puente Formation, Fernando Formation, San Pedro Formation, La Habra Formation, alluvial and colluvial deposits (7.8–0 Ma)

The Yorba Member of the Puente Formation is a thinly bedded siltstone with a subordinate proportion of sandstone. The overlying Sycamore Canyon conglomeratic sandstone and the Yorba siltstone have been mapped at the surface as separate units, but, south of the Whittier fault in the subsurface, thick sandstone beds in the Yorba Member can be distinguished from the Sycamore Canyon sandstone only by microfaunas. In isolated outcrops, lithologic similarities between siltstone of the Yorba and La Vida Members make distinction between those two units based on lithologic characteristics difficult (Siang Tan, personal communication).

Individual sandstone bodies of the Sycamore Canyon and Yorba Members are elongated east–west and pinch out updip in the footwall block of the Whittier fault at the Brea–Olinda oil field (Yeats and Beall, 1991). An isopach map showing the total thickness of the Sycamore Canyon and Yorba Members reflects the predominantly east–west trend of the individual sandstone units (Fig. 4). This sandstone body architecture has been interpreted to indicate the location of a Late Miocene, turbidite fan-channel system (Redin, 1991). The distribution pattern of the Yorba and Sycamore Canyon Members is consistent with the presence of contemporary bathymetrically high areas that were predecessors to the structurally elevated Puente and Chino Hills on the north and the Coyote Hills on the south. Such sea floor elevations, possibly anticlinal culminations, were early indications of horizontal contraction that was, at least in part, associated with movement on the Whittier fault. Sandstone and siltstone of the Pliocene Fernando Formation and shallow marine and nonmarine Pleistocene and Recent sand, silt and gravel crop out on the flanks of the Whittier structure and record the transition from deep-water turbidite deposition to the present coastal plain depositional environment.

3. Structural framework

The main structural elements of the study area are the

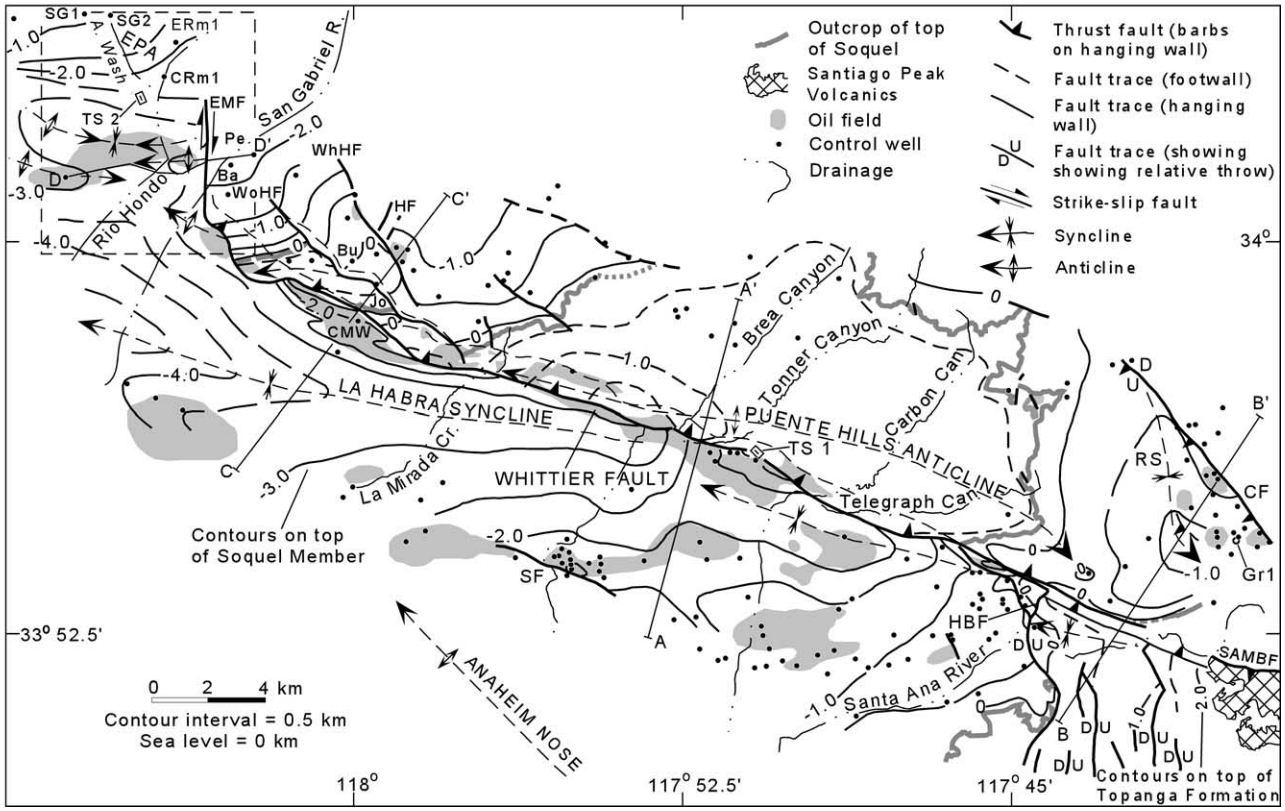

Fig. 5. Structure contour map on the top of the Soquel Member of the Puente Formation except east of the Horseshoe Bend fault and south of the Whittier fault where contours are on the top of the Topanga Formation. Contours are short-dashed where projected above ground level and long-dashed where not well constrained. Dashed box is location of Fig. 9b. Chino fault (CF), East Montebello fault (EMF), Elysian Park anticline (EPA), Handorf fault (HF), Horseshoe Bend fault (HBF), Ridge syncline (RS), Santa Ana Mountain Boundary fault (SAMBF), Stearn fault (SF), Whittier Heights fault (WhHF), Workman Hill fault (WoHF), California Time Petroleum Grayco 1 (Gr1), CalResources Rosemead 1 (CRm1), Chevron Murphy–Whittier 304 (CMW), Conoco Buehler 1 (Bu), Exxon San Gabriel Units 1-1 (SG1) and 1-2 (SG2), Los Angeles Brewing Jones Community 1 (Jo), Shell Bartola 1 (Ba) and Pellissier 1 (Pe), Alhambra Wash trench site (TS 2), Olinda Creek trench site (TS 1). Lines A–A′, B–B′, C–C′ and D–D′ are locations of cross-sections in Figs. 6–8 and 9a, respectively. Outcrop of top of Soquel modified from Durham and Yerkes (1964), Yerkes (1972) and Schoellhamer et al. (1981). See Fig. 1 for location of map in the Los Angeles basin and Fig. 3 for names of oil fields.

Puente Hills anticline, the La Habra syncline and the Whittier fault system in which the Whittier fault cuts the crest and the steeply dipping southern limb of an asymmetric anticline along a 40 km strike-length (Fig. 5). We divide the Whittier fault into three structurally distinct segments, a southeastern segment, a central segment and a northwestern segment. Faults and folds that are probably related to changes in stratigraphy and to changes in structural style complicate the southeastern and northwestern segments. The Whittier fault ends in the northwest as a north-trending, dextral strike-slip fault. The termination of the Whittier fault in the southeast is obscure because of extensive alluvial cover and a lack of wells as well as because of the complicating effects of the uplift of the Santa Ana Mountain block, which we discuss below. Four representative cross-sections (Figs. 6–9), which are integrated with structural contour maps and a cross-section network (Bjorklund, in preparation), illustrate the structural features in the three segments.

3.1. Central segment: Sansinena, Brea–Olinda and Yorba Linda oil fields

The central segment of the Whittier fault extends for 18 km from Telegraph Canyon to La Mirada Creek and forms the southern boundary of the structurally coherent crestal part of the Puente Hills anticline (Fig. 4). Because of a relative lack of complexity and an abundance of wells in this central segment, we have been able to construct highly resolved cross-sections that we suggest are crucial to understanding the evolution of the Whittier fold–fault system. In cross-section A–A′ (Fig. 6), well and surface geologic data constrain the structural and stratigraphic relationships to the depth of the Soquel Member of the Puente Formation in the footwall block and to the depth of the Topanga Formation in the hanging wall block. Below well depths, the thicknesses of the strata have been interpreted from wells off the line of section and from outcrops in the Santa Ana Mountains. The geometric relationships of units below well depths and near the Whittier fault follow directly from the structural model

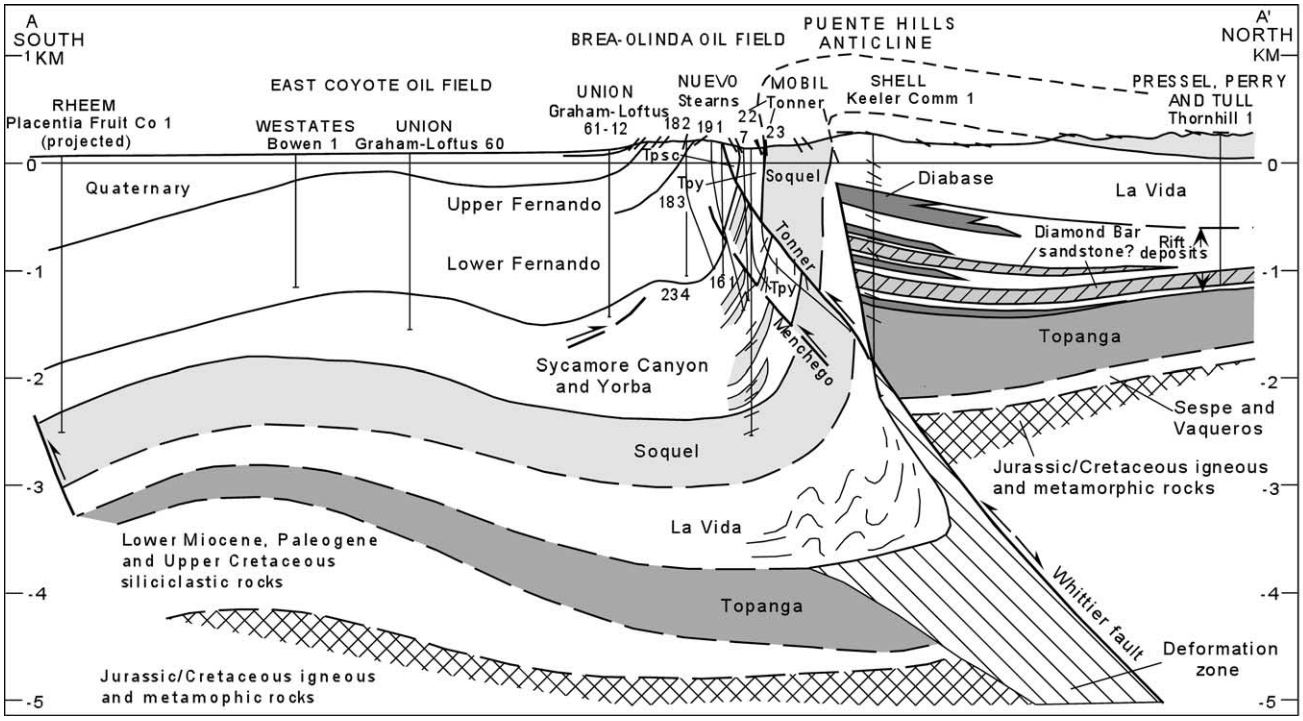

Fig. 6. Cross-section A–A′ of the central segment of the Whittier fault across Brea–Olinda oil field. Correlations modified from Durham and Yerkes (1964), Yeats and Beall (1991) and unpublished data from Aera Energy LLC (formerly Shell Oil Company). Interpretation of footwall block of the Whittier fault based on data from Chevron Murphy–Coyote No. 373 in West Coyote Oil Field (West and Redin, 1990; McCulloh et al., 2000) and Prado Petroleum Government 165-1 east of the Chino fault (Fig. 1) and the extrapolation of outcrop data from the Santa Ana Mountains (Schoellhamer et al., 1981). Stippled units in Sycamore Canyon and Yorba members represent oil-productive, turbidite fan-channel sandstones. The deformation zone is discussed in Appendix A. Long-dashed contacts are approximately located. Short-dashed contacts are extrapolated above ground level. The double arrows on the Whittier fault indicate slip directions of separate phases of deformation. Sycamore Canyon Member (Tpsc), Yorba Member (Tpy). See Fig. 5 for location of cross-section.

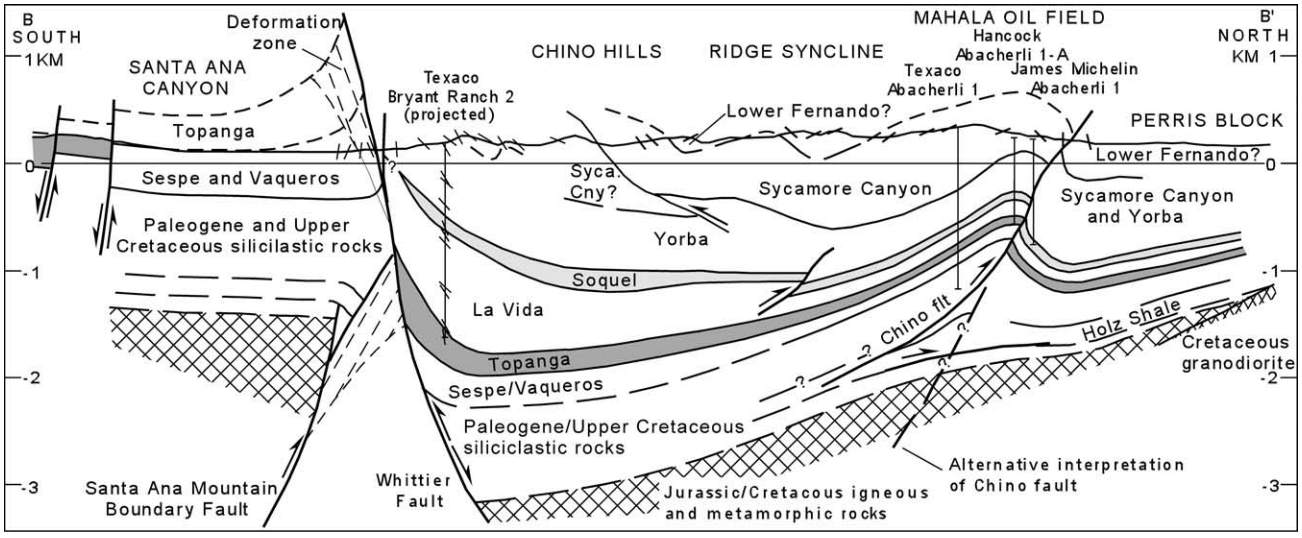

Fig. 7. Cross-section B–B′ of the southeastern segment of the Whittier fault across Santa Ana Canyon. Interpretation of hanging wall block of Santa Ana Mountain Boundary Fault (footwall block of Whittier fault) is based mainly on surface mapping of Durham and Yerkes (1964) and Schoellhamer et al. (1981) and wells not on section. Interpretation of hanging wall block of Whittier fault below well depths based on the thickness of the Cretaceous sequence in Prado Petroleum Government No. 165-1 well (Lang, 1978) (Fig. 1), located 3.3 km southeast of the section line, and the extrapolation of outcrop data from the Santa Ana Mountains. The base of the Lower Fernando Member is approximately located with unpublished microfaunal data (Aera Energy LLC) from Grayco Oil Grayco No. 1 well. See Fig. 5 for location of cross-section and explanation of symbols.

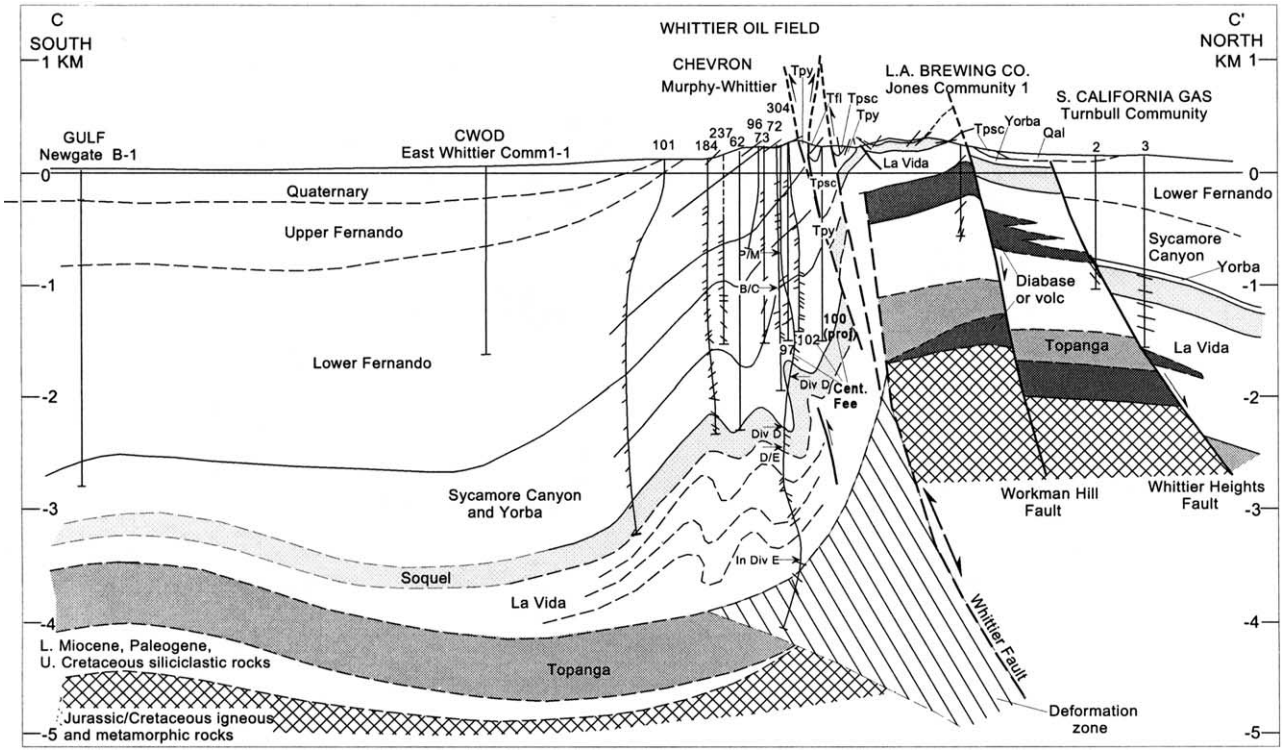

Fig. 8. Cross-section C–C′ of the northwestern segment of the Whittier fault across Whittier Oil Field. Microfaunal divisions (Division E (E), Division D/Division E contact (D/E), Division D (D) and Division B/Division C contact (B/C)), Yorba Member (Tpy), Sycamore Canyon Member (Tpsc), Pliocene/Miocene contact (P/C), Lower Fernando Member (Tfl). Arrows along the wellbore identify locations of microfaunal data. Cross-section modified from Yerkes (1972; cross-section C–C′) and Herzog (1998; cross-section C–C′). Interpretation of hanging wall block based on data from Daviess and Woodford (1949). The two volcanic or diabase units are each drilled by a single well (Los Angeles Brewing Jones Community 1 and Conoco Buehler 1) (Fig. 5). Woodford et al. (1944) reported Luisian and Relizian foraminifera in the latter well. Since the 3-D shape of these igneous units is not known, the interpretation on the cross-section is speculative. See Fig. 5 for location of cross-section and explanation of symbols.

described in Appendix A and result in a balanced cross-section (See also Fig. 8 in Section 3.3).

The Shell Keeler Community No.1 well (Fig. 4) penetrated the thickest section of the La Vida Member in the study area. That greater thickness results from the sandstone, siltstone and diabase intrusions in the lower part of the La Vida Member (Fig. 6) that are only found north of the Whittier fault. The base of the La Vida Member in cross-section A–A′ has been drawn so that thickening of the La Vida Member in the core of the syncline compensates for attenuation of the La Vida Member in the steeply-dipping forelimb (refer to Appendix A for details). A small, secondary fold shown on the forelimb, the shape of which is derived from well data, is attributed to layer-parallel shortening that has been accommodated by localized folding and thrusting. The presence of a bedding-plane thrust has been inferred (cf. Brown, 1988; Narr and Suppe, 1994; Herzog, 1998). Well and surface data establish the steep dip of the main Whittier fault to a depth of about 2 km. Conservation of bed length and area of the sedimentary layers in cross-section require the dip of the fault to be approximately 50–55° within the basement (cf. Cook, 1988, p. 58; Appendix A). The Tonner and Menchego forelimb faults have been delineated by well data and also dip 50–55° to the north.

We interpret the lower part of the La Vida Member that contains interbedded diabase sills, the Diamond Bar sandstone and siltstone to be made up of rift-fill that formed in a Middle to Early Late Miocene half-graben antecedent to the establishment of the presently active Whittier fault. We base this interpretation on the following observations:

1. The location and triangular shape of the thick area of the La Vida Member north of the Whittier fault (Fig. 3).
2. The wedge-shaped cross-sectional geometry of the lower La Vida Member (Fig. 6).
3. The likely intrusion of the diabase along the Whittier fault (Durham and Yerkes, 1964, p. 23), indicating lithospheric extension.
4. The presence of the diabase sills and sandstone only north of the Whittier fault (Durham and Yerkes, 1964, p. B23; Yerkes, 1972, p. C11).

The graben-bounding fault is here named the proto-Whittier normal fault. We will show that structural inversion of the wedge-shaped rift-fill along the proto-Whittier fault produced the Puente Hills anticline, with gently dipping Upper Miocene beds on the crest and northern limb and a steeply dipping forelimb (Fig. 6), as well as many of the other features that characterize the present Whittier fold–fault system.

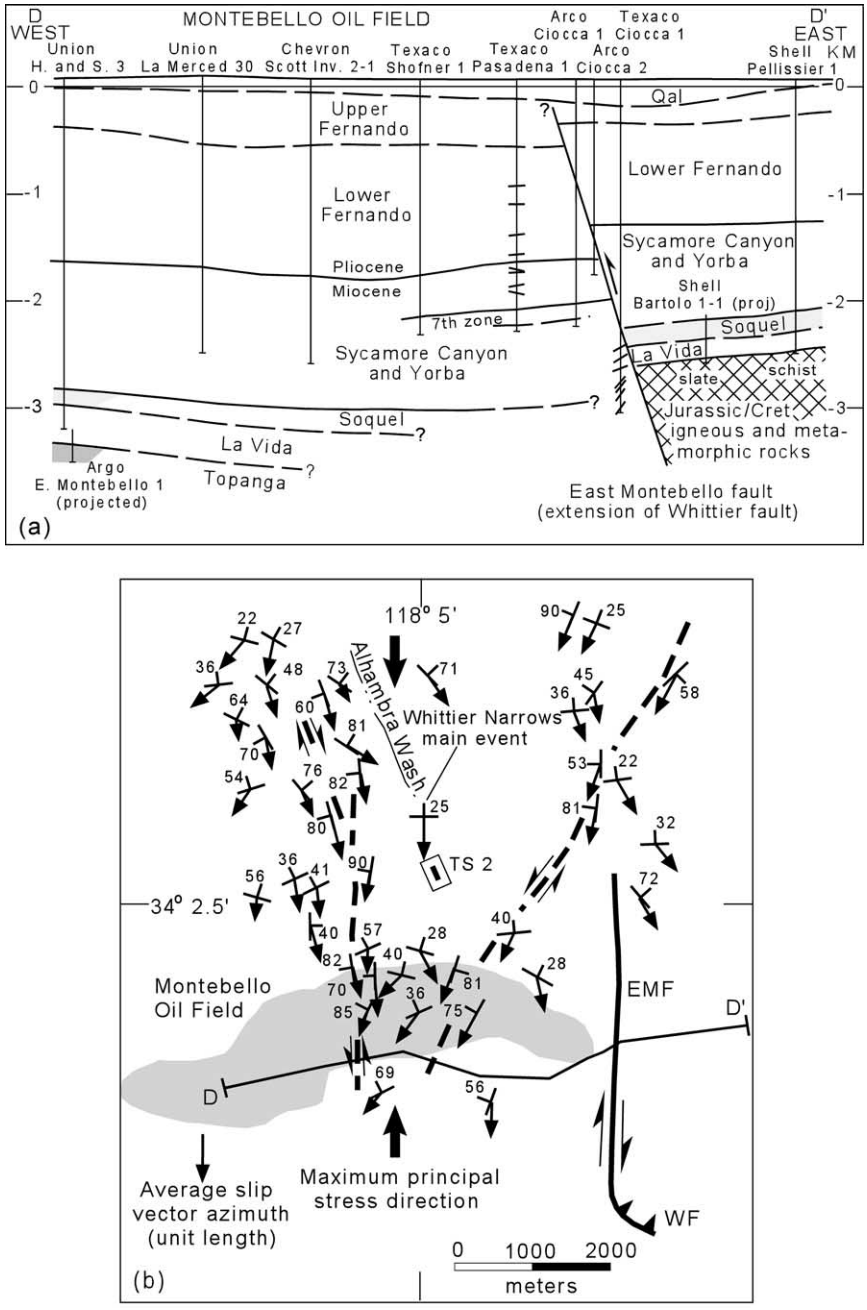

Fig. 9. Cross-section and map at northwestern end of the Whittier fault. (a) Cross-section D–D′ of the East Montebello fault (north-striking extension of Whittier fault). According to well reports, basement is slate (Santa Monica slate?) in Shell Bartola One-No. 1 redrill and fractured metamorphic rock (faulted Santa Monica slate?) in Shell Pellissier No. 1 (Fig. 5). Correlations are modified from Yeats and Beall (1991), Yeats and Huftile (1997) and Oregon State University unpublished data. See Figs. 5 and 9b for location of cross-section. (b) Map of epicenters of Whittier Narrows earthquake (1987, M = 5.9) and aftershocks. Focal mechanisms and maximum principal stress data are from Hauksson and Jones (1989). Symbols showing strike and dip of focal planes are gray. Arrows are horizontal projections of slip vectors of unit length and proportional to plunge angle, i.e. if the plunge angle is 0°, the horizontal projection is unit length. Dashed strike-slip fault symbols show approximate alignments of strike-slip focal mechanisms. East Montebello fault (EMF), Whittier fault (WF), Alhambra Wash trench site (TS 2). See Fig. 5 for location of map in study area.

3.2. Southeastern segment: Esperanza oil field to Santa Ana River

The southeastern segment of the Whittier fault zone extends for 9 km, from Telegraph Canyon to the Santa Ana River and exposes, in the vicinity of the Santa Ana Canyon, the Santiago Peak Volcanics (ca. 135 Ma), the oldest rocks of the footwall block that crop out in the area (Fig. 5). An understanding of the structural relationships in this segment is important in establishing the structural style of the Topanga sandstone and older units down-plunge to the NW. The Horseshoe Bend fault is one of several

north-trending, east side up, faults that have been mapped on the west-dipping flank of the Santa Ana Mountains (Schoellhamer et al., 1981; Fig. 5). These faults, which reflect differential vertical uplift of the Santa Ana Mountains, do not cross the Whittier fault. For that reason, the aggregate sense of vertical separation of the northern and southern sides of the Whittier fault changes at the Horseshoe Bend fault (cf. Heath, 1954; Durham and Yerkes, 1964; Tan et al., 1984). Northwest of the Horseshoe Bend fault, outcrops indicate that the vertical separation of the Whittier fault is north-side-up; southeast of that fault, the vertical separation is north-side-down, because of the effect of uplift on the eastern side of the Horseshoe Bend fault (Figs. 5 and 7). The horizontal separation of outcrops of Topanga and undifferentiated Sespe and Vaqueros strata in Santa Ana Canyon is right-lateral (Durham and Yerkes, 1964, p. B31 and Plate 1). We interpret the right-lateral separation to be mainly a relict of earlier normal movement on the proto-Whittier fault, which offset the Topanga Formation and older rocks and resulted in a thicker La Vida Member north of the fault than south of the fault (cf. Harding, 1990, pp. 1594–1595; Figs. 6 and 7). This interpretation implies that the Whittier fault trace in Santa Ana Canyon, although certainly affected by later displacements, is an exhumed segment of the proto-Whittier normal fault. Extensive trenching has revealed that thick, chaotic deposits of colluvium and alluvium and landslide blocks cover the Whittier fault trace in this area (Hannan et al., 1979). The results of the trench study were inconclusive with regard to sense of slip on the Whittier fault. Steeply south-dipping to overturned Topanga and undifferentiated Sespe and Vaqueros beds, on the northern limb of the La Habra syncline, have been mapped in the Santa Ana canyon by Heath (1954), Durham and Yerkes (1964) and Tan et al. (1984) and are represented in Figs. 5 and 7. Down-plunge to the northwest, Upper Miocene and Pliocene beds dip steeply to the south or are overturned in the footwall block of the Whittier fault (Figs. 6 and 8). Taken together, the structural features observed in these younger beds to the NW and the older strata in Santa Ana Canyon are compatible with structural deformation in the footwall block as a result of reverse slip on the Whittier fault. We suggest that the steeply south-dipping Topanga and undifferentiated Sespe and Vaqueros strata in Santa Ana Canyon provide critical evidence showing that reverse slip developed on the southeastern segment of the Whittier fault before the uplift of the Santa Ana Mountains.

Poorly exposed faults and steeply dipping to overturned beds that characterize the outcrops of the Topanga and undifferentiated Sespe and Vaqueros strata in Santa Ana Canyon indicate structural complexity. We have designated areas on cross-sections in the synclinal core of the footwall block that we interpret to be characterized by similar structural complexity as deformation zones (see Appendix A). East of the Topanga and undifferentiated Sespe and Vaqueros outcrops in the Santa Ana Canyon area, extensive alluvial cover obscures the Whittier fault. On the northern end of the Santa Ana Mountains, data from wells and outcrops indicate that strata, although disrupted by faults, generally dip steeply to the north (Schoellhamer et al., 1981). The structural and stratigraphic interpretation below the undifferentiated Sespe and Vaqueros Formations shown in Fig. 7 is based on the down-structure projection of these data. We have interpreted, on the basis of the north-dipping beds on the northern end of the Santa Ana Mountains, the deeper structure to be associated with a south-dipping, blind reverse fault, here named the Santa Ana Mountain boundary fault (SAMBF in Figs. 5 and 7). Most published interpretations project the Whittier fault to the southeast across the Santa Ana River flood plain to join the SAMBF, which has been mapped from the Temescal Valley as a segment of the right-lateral Elsinore strike-slip fault (cf. Gray, 1961; Schoellhamer et al., 1981). Reasonable estimates of cumulative slip on the northern Elsinore fault range from 10 to 15 km since 2.5 Ma, possibly the maximum age for the fault segment The zone of seismic activity along the Elsinore fault zone ends south of the Santa Ana River, and the location of the northward extension of the Elsinore fault is problematic because of lack of seismicity and Quaternary cover. The Elsinore fault zone could merge with the Whittier fault by changing strike from NW to WNW. Alternatively, by means of right step-overs that are characteristic of its trace to the southeast, the Elsinore fault could continue to the NW and merge with the buried Central Avenue fault (Greenwood and Morton, 1991) located within the alluvial covered valley east of the Chino fault (Fig. 1). We suggest that the extension of the Whittier fault across Santa Ana canyon and the Santa Ana Mountains to join the Elsinore fault is not compatible with the observed shallow structures; the south-dipping beds in the footwall of the Whittier fault and the north-dipping beds in the Santa Ana Mountains. We interpret the structural relationships in Santa Ana Canyon to reflect interactions of conjugate faults, the SAMBF on the south and the Whittier fault on the north (Fig. 7). Subsequent to reverse movement on the Whittier fault in the Santa Ana Canyon area, uplift on the SAMBF produced the north-dipping beds observed at outcrop on the northern end of the Santa Ana Mountains. That uplift also accounts for the north-dip of beds north of the Whittier fault in the Chino Hills (Fig. 7). The SAMBF is interpreted to extend to the northwest at least as far as the Horseshoe Bend fault. The easternmost extent of the Whittier fault cannot be defined on the basis of the data available to this study.

The main structures in the hanging wall block of the southeastern segment of the Whittier fault are the Ridge Syncline and the Chino fault and anticline (Fig. 7). Small folds at shallow depths are interpreted to be associated with bedding-plane thrusts. The Chino fault is a southwest-dipping reverse fault at shallow depths (Durham and Yerkes, 1964). We interpret the throw of the Chino fault at the level of the Topanga sandstone to be about 200 m near the crest of the Mahala oil field anticline (Fig. 7). Below

well depths the dip of the fault is not known. The fault could either flatten and die out, e.g. in the Holz Shale Member, or it could dip from steeply southwestward to vertical and offset basement rocks. Both alternatives are shown in Fig. 7. Resolution of the correct interpretation awaits further study of the relationship between the Chino fault and the Elsinore fault farther to the southeast.

3.3. Northwestern segment: Whittier oil field to San Gabriel River (Whittier Narrows)

The northwestern segment of the Whittier fault extends for 15 km from La Mirada Creek to the Whittier Narrows (Fig. 5). The northwesternmost exposure of the fault is in Turnbull Canyon, just north of Whittier, California. At that location, the La Vida Member is juxtaposed against the Sycamore Canyon Member (Yerkes, 1972). Farther northwest, alluvial deposits cover the projected trace of the Whittier fault, but well data from the Rideout Heights and Montebello oil fields constrain the location of the fault as far north as the San Gabriel River (Yeats and Huftile, 1997; Herzog, 1998). At Rideout Heights, the covered extension of the trace of the Whittier fault bends sharply, from N70W to nearly N–S, to become the East Montebello fault (Wright, 1991, p. 49; Herzog, 1998).

The footwall and hanging wall blocks of the northwestern segment are structurally complex at the Whittier oil field (Fig. 8). Well data, including dipmeter readings, indicate that the Soquel Member is folded in the core of the footwall block (Herzog, 1998). Based on observations of the style of deformation in outcrops in the hanging wall block of the Whittier fault and data from the dipmeter in the Chevron Murphy–Whittier No. 304 well, the La Vida Member is interpreted to have been intensely folded (Fig. 8). Faults that branch from the main Whittier fault offset forelimb beds. The Chevron 304 well, the deepest well along the length of the Whittier fault, is the only well to have penetrated the Topanga sandstone in the footwall block close to the fault, except for some shallow wells near Santa Ana Canyon. Wells in the hanging wall block at the Whittier oil field are relatively shallow, and none reaches crystalline basement. The locations and attitudes of the two normal faults shown in Fig. 8, the Workman Hill and the Whittier Heights Faults, are determined at shallow depths from outcrops and wells (Fig. 5). The structural interpretation of the hanging wall block below well depths is less well constrained than that in the area of the central segment of the fault, cross-section C–C′ (Fig. 8).

At the San Gabriel River, the Whittier fault dips steeply to the east to a depth of at least 3 km (Fig. 9a). Reverse separation at the top of the Miocene is 320 m. Except close to the fault zone, simple homoclinal dip characterizes the structures in the footwall and hanging wall blocks. Structure contours on the top of the Soquel Member indicate that the East Montebello fault terminates about 3 km north of the San Gabriel River (Fig. 5). We follow Wright (1991) in interpreting the East Montebello fault as primarily a strike-slip fault.

Topographic lineaments and small faults temporarily exposed in a trench study north of the San Gabriel River near the Alhambra Wash (Figs. 5 and 9b) have been cited as evidence that the Whittier fault extends to the northwest across the Whittier Narrows (Bullard and Lettis, 1993; Gath et al., 1994), but such extension would require a westward bend of the Whittier fault, which is not evident in the subsurface data. If an extension does exist, well data suggest that the apparent total vertical separation on the extension would be less than 50 m at the top of crystalline basement (see Fig. 5 for well locations).

4. Direction of tectonic transport on the Whittier fault

4.1. Previous studies of displacements along the Whittier fault

A fundamental problem in the Los Angeles basin is the relative role of dextral strike-slip and reverse slip on the Whittier fault. Vertical separation on the Whittier fault of over 4 km is generally accepted (cf. Yerkes, 1972, p. 29). The consensus on the amount of horizontal separation is not so evident. Estimates of long-term, dextral strike-slip displacement range from 0 to 40 km (English, 1926; Gourley, 1975; Sage, 1975). A correlation of the Horseshoe Bend fault with a fault north of the Whittier fault at Scully Hill (Santa Ana Canyon area) suggests a post-Middle Miocene movement of about 4.6 km (Woodford et al., 1954). In this study, the Horseshoe Bend fault has been shown to be restricted to the south side of the Whittier fault, precluding correlation with the fault at Scully Hill. Offsets of drainage courses of 1.2–1.5 km at Brea Canyon and Tonner and 2.7 km at Carbon and Telegraph Canyons have been cited as evidence of right-lateral strike-slip movement along the Whittier fault (Hill, 1954; Durham and Yerkes, 1964; Yerkes, 1972). Davis et al. (1989) argued that consistent offsets of drainages are not observed on all similar stream courses, and many deflections seem to be related to local structure rather than to the Whittier fault. The three largest drainages, Rio Hondo, the San Gabriel River and the Santa Ana River, do not show offsets that could have been caused by right-slip on the Whittier fault. English (1926) attributed stream offsets entirely to differential erosion of softer rocks along the Whittier fault. Lamar (1961) estimated 30 km of post-Paleocene (post ca. 55 Ma) dextral strike-slip by comparing thickness distributions of the upper Silverado Formation on opposite sides of the Whittier and Elsinore faults. Sage (1975) postulated 40 km of dextral strike-slip on the Whittier and Elsinore faults to explain the apparent offset of the Paleocene shoreline. Large offsets of 30–40 km are not compatible with the late Pliocene (2.5 Ma) origin now ascribed to the Elsinore fault (Hull and Nicholson, 1992) and may be related to a

different kinematic regime. Gourley (1975) concluded that lithofacies maps of Upper Miocene rocks near the Whittier oil field do not require strike-slip movement on the Whittier fault but could accommodate up to 750 m of offset. Wright (1991) pointed out an apparent 8 km, right-lateral offset of thick Soquel sandstones along the southeastern part of the Whittier fault, but he recognized that the depositional pattern of the Soquel may have been non-linear and strongly influenced by structural features that were not related to the Whittier fault. McCulloh et al. (2000) analyzed thickness trends of an isopach map of Paleogene strata to estimate 8–9 km of dextral strike-slip on the Whittier fault since the Paleogene. Our analysis of their data leads us to conclude that their isopach map is not a unique interpretation of the data and is equivocal in determining the kinematics of the Whittier fault. Determinations of fault displacements that rely on piercing points defined by the extrapolation of subsurface facies trends are inherently likely to lead to estimates with large degrees of uncertainty. The amount of that uncertainty could well be as great as the estimated offset itself.

Numerous paleoseismic studies have been carried out along the Whittier fault by excavating trenches. Two studies of trench profiles have embodied conclusions about the transport direction. At Olinda Creek on the central segment of the Whittier fault in Brea–Olinda oil field, Gath et al. (1992) concluded that Quaternary channel sandstones (10–12 Ka) had been offset 9–26 m in a dextral strike-slip sense and estimated a minimum slip rate of 2.8 mm/year on two faults. They estimated the ratio of lateral to vertical slip at 12:1. Radiocarbon dates indicate that faulting at the Olinda site took place within the past 17,000 years. Their correlation of three, laterally separated sand bodies on the south side of the fault with a vertically-stacked group of sand bodies on the north side is inferred from partial exposures in trenches, but distinguishing characteristics and ages of the sand bodies facilitating correlation across the fault are not clearly established. From a trench study near Alhambra Wash in the Whittier Narrows, Gath et al. (1994) estimated 3 m of vertical displacement and 6–10 m of dextral strike-slip on a fault trending approximately N20W that was postulated to be an extension of the Whittier fault. However, the distribution of the channel sandstone on the upthrown side of the fault is discontinuous and the location of the channel edge is ambiguous on both sides of the fault.

Our review of previous studies of displacements on the Whittier fault suggests to us that a strike-slip transport direction has not been unequivocally established. Sources of possible errors in all of the studies are uncertainties in across-the-fault correlations and poorly constrained piercing points. The ranges of error attributed to these uncertainties seem to be understated. Our 4-D analysis of the available data shows that although a small component of strike-slip separation is required, dip-slip separation has been predominant on the Whittier fault during most of the past 8 My. Our analysis does not, however, preclude the possibility of a small amount of predominantly strike-slip movement along the southeastern part of the Whittier fault in the late Quaternary.

4.2. A null hypothesis

A main aim of this paper is to illustrate the way in which high spatial-resolution data can be used to work out the 3-D characteristics and geologic history of a relatively small volume (ca. 2000 km^3) of deformed continental rocks at shallow depth. In conjunction with this objective, we examine the relative roles of strike slip and dip separation on the Whittier fault by making an estimate of the direction of tectonic transport along the Whittier fault. Here, we simply advance a null hypothesis to explain why our estimates of horizontal contraction have been made assuming a N–S direction of tectonic transport, viz. "*The azimuth of tectonic transport indicated by the mechanism of the most recent large earthquake closest to the Whittier fault, which was the Whittier narrows earthquake of 1987, is representative of the mean direction of tectonic transport on the Whittier fold–fault system over the past ca. 8 My*".

To the extent that we can find evidence of motion with other azimuths, we are ready to modify the null hypothesis. So far, this has not proved necessary, but we point out that most papers cited in the introduction to this section have concluded that the tectonic transport direction on the Whittier fault has been predominantly N70W, parallel to the fault's strike, rather than, as we have concluded, N–S.

4.3. The shortening azimuth from earthquakes as consistent with that from mapping

Data from earthquakes (Hauksson and Jones, 1989) indicate a present, generally north-to-south tectonic transport direction for the hanging wall block of the northwestern segment of the Whittier fault with respect to the footwall block. The Whittier Narrows earthquake (1987, $M = 5.9$), which occurred on a thrust that dips 25° north just west of the Whittier fault, is the closest large, historic earthquake to the Whittier fault. The slip direction of the main event was N–S. Aftershocks of the main event with steeply dipping, strike-slip focal mechanisms ranging in depth from 10 to 15 km suggest that conjugate faults bound the aftershock cluster on its eastern and western sides (Hauksson and Jones, 1989). The main event and all of the aftershocks, 43 of which are shown in Fig. 9b, are located west and northwest of the Whittier and East Montebello faults. The average slip-vector azimuth of the main event and the aftershocks taken together is also N–S, establishing a N–S tectonic transport direction for a crustal block adjacent to the Whittier fault.

Focal mechanism data from the 1987 earthquake and large-scale structural relationships in the hanging wall block of the Whittier fault are not compatible with strike-slip movement on a fault with a strike of N70W, but they are

consistent with a predominantly N–S tectonic transport direction. The hanging wall block of the northwestern segment of the Whittier fault overrides the footwall block to the west and south with reverse separation (Figs. 5, 8 and 9a). Any significant amount of dextral strike-slip movement along the Whittier fault with its N70W strike would have produced normal movement on the East Montebello fault, which is not observed. The structural coherence of the leading edge of the Whittier fault, i.e. the absence of pull-apart features along strike, that has emerged from our work and is best displayed in the structure map on the top of the Soquel Member (Fig. 5), is consistent with a N–S transport direction along the entire length of the Whittier fault.

5. Inversion history of the Whittier half-graben

We recognize three phases in the evolution of the Whittier fold–fault system. The three phases are illustrated by balanced and restored cross-sections that represent time slices of the Whittier structure at 7.8 Ma, 1.0 Ma and the present (Fig. 10; Appendix A).

5.1. Formation and sedimentary infilling of a half-graben (16–7.8 Ma)

Cross-section A–A′ (Fig. 6) across Brea–Olinda oil field has been restored to 7.8 Ma to illustrate the end of the rifting phase (Fig. 10a). The restoration represents removal of fault offsets and folds by down-dip translation of the hanging wall block parallel to the dip of the fault in crystalline basement until the top of the Soquel Member is horizontal, which is assumed to have been its attitude at the time of deposition (see Appendix A for details). The depths are uncorrected for compaction and regional westward tilt. The overall effect of decompaction of the sedimentary section and the removal of the regional tilt would be to increase the depths shown by more than 1 km.

Although the extrusion of the Glendora Volcanics (ca. 16–14 Ma) is the earliest indication of rifting in the region, the presence of the Diamond Bar sandstone in the lowermost part of the La Vida Member is taken as evidence of the earliest movement on the proto-Whittier normal fault and the beginning of the formation of the Whittier half-graben (ca. 14 Ma). The distribution and thickness of the Soquel Member appears to have been unaffected by penecontemporaneous faulting, and extensional movement on the proto-Whittier fault is, therefore, inferred to have ceased before the end of deposition of the La Vida Member of the Puente Formation (9.4 Ma) (Barron and Isaacs, 2001). We can speculate that the stratigraphically highest diabase sill in the La Vida siltstone may approximately mark the tip line of the graben-forming fault and the top of the rift deposits. Assuming that magma was intruded along the graben-forming normal fault and spread laterally to form the diabase sills, then the absence of sills higher in the section can be interpreted to indicate the absence of a fault that could act as a migration pathway for the magma. The Topanga sandstone was downthrown to the northeast by more than 1 km along the proto-Whittier normal fault.

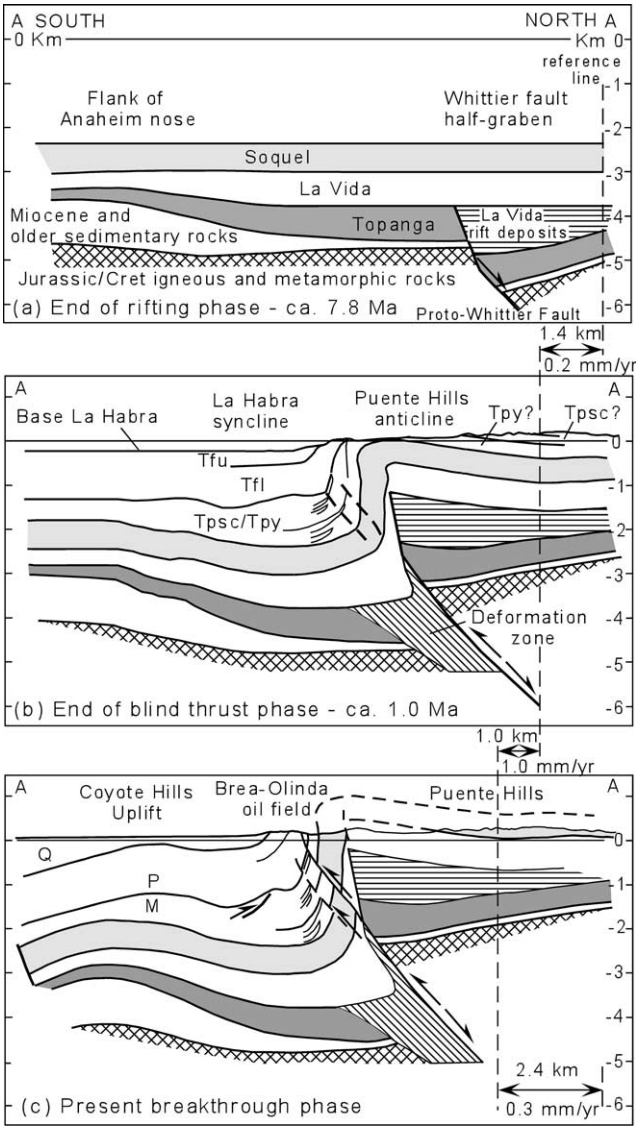

Fig. 10. Cross-section A–A′ across the central segment of the Whittier fault with restorations at 7.8 Ma (Fig. 10a), 1.0 Ma (Fig. 10b) and 0.0 Ma (Fig. 10c), showing the three-phase evolution of the fault. The amount (km) and rate (mm/year) of horizontal contraction is shown for each time-slice with respect to a reference line fixed to a point on the top of the Soquel Member. Yorba Member (Tpy), Sycamore Canyon Member (Tpsc), Miocene (M), Pliocene (P), Lower Fernando Member (Tfl) and Upper Fernando Member (Tfu). See Fig. 6 for details of Fig. 10c.

5.2. Inversion of the half-graben and uplift of the Puente Hills above a blind reverse fault (7.8–1.0 Ma)

Cross-section A–A′ (Fig. 6) across Brea–Olinda oil field has been restored to ca. 1.0 Ma to illustrate a late stage in the uplift of the Puente Hills (Fig. 10b). The restoration represents removal of throw on the forelimb faults by rigid-body movement parallel to fault dip, followed by removal of

folding of the base of the La Habra Formation along restoration vectors parallel to the dip of the faults (cf. Novoa et al., 2000). Dashed lines approximate the future locations of the forelimb faults on the restored section. Displacement in the subsurface on these faults may have already begun at 1.0 Ma. The topographic elevation shown in the area of the Puente Hills has been inferred because it is needed to provide a local source for the Miocene clasts that are present in the Pliocene and Pleistocene strata (Yerkes, 1972). Because all beds that overlie the Soquel Member have been eroded from the crest of the Puente Hills anticline, the thicknesses shown for those units on the restored cross-section are conceptual.

Contractional reactivation of the Whittier half-graben began with rigid displacement of the wedge of rift deposits and the underlying older sedimentary and crystalline basement rocks along the proto-Whittier fault. Fault displacement was dissipated in the cover units by folding that produced a linear, bathymetric high on the sea floor, which would later become the Puente Hills anticline. At the Brea–Olinda oil field, the Lower Fernando Formation (ca. 5.3–2.5 Ma) unconformably overlies Yorba siltstone (ca. 7.8–7.1 Ma) in Aera Energy LLC Puente B-32 (Fig. 3) (Aera Energy LLC, unpublished data). The section of Yorba and Sycamore Canyon siltstone and sandstone thickens southward toward the axis of the La Habra syncline (Figs. 4, 6 and 10b). These relationships indicate that shortening in this part of the Los Angeles basin had begun as early as ca. 7.8 Ma.

5.3. Breakthrough of the Whittier blind reverse fault onto the seafloor and subsequent uplift (1.0 Ma–present)

The end of the Whittier blind reverse-fault phase occurred when faults emanating from the master fault broke through the entire sedimentary section and reached the seabed (Fig. 10c). The time of breakthrough is not well constrained. The presence of diabase and Puente Formation clasts in a basal Lower Fernando conglomeratic bed has been cited as evidence for surface faulting as early as 5.1 Ma (Yerkes, 1972, pp. C15, C29). However, if the diabase in the La Vida Member were exposed and being eroded from the hanging wall block of the Whittier fault at 5.1 Ma, then subsequent uplift and erosion would have exposed Jurassic rocks in the Puente Hills today. The oldest unit that crops out near the Brea–Olinda oil field is a Miocene age diabase sill in the La Vida Member. We speculate that the source of the diabase fragments in the Fernando Formation more likely was located in the Santa Ana or San Gabriel Mountains and has been eroded.

A decrease in the rate of rotation of the beds in the forelimb, which might correlate with fault breakthrough, is indicated by an angular unconformity (ca. 2.5 Ma) between the upper and lower members of the Fernando Formation near Brea Canyon (Yerkes, 1972; Tan et al., 1984; Blake, 1991). However, based on our restoration of cross-section A–A′, no fault breakthrough at the surface is necessary to accommodate displacement along the Whittier blind fault before Early Pleistocene. The lower units of the La Habra Formation are folded on the forelimb of the Puente Hills anticline (Yerkes, 1972). Assuming that breakthrough occurred after folding of the La Habra beds, the time of breakthrough is estimated at ca. 1.0 Ma, although small faults along the anticline may have existed earlier.

Along the strike-length of the Whittier fault, the geometric relationships among the proto-Whittier fault, the blind reverse fault and the breakthrough faults are complex. At the Brea–Olinda oil field, the breakthrough fault, the Tonner fault, is generally aligned with the trajectory of the Whittier blind reverse fault (coincident with the earlier proto-Whittier normal fault) and merges with it at about 1.5 km depth, near the top of crystalline basement (Figs. 6 and 10c). Northwest from the Brea–Olinda oil field to the Whittier Narrows, the breakthrough fault is steeply dipping and cuts across the crest of the Puente Hills anticline, reaching the backlimb (Fig. 5). At the Whittier oil field several forelimb and crestal faults that offset rocks as young as Lower Pliocene in age (ca. 5.0 Ma) are exposed at the surface, but their geometric relationships with the Whittier blind reverse fault are not well constrained by the limited data (Fig. 8). Our interpretation for the Whittier oil field area is that the breakthrough faults are aligned with the upward trajectory of the shallow segment of the Whittier blind reverse fault. At Santa Ana Canyon, the section in which the breakthrough fault might have been recognized has been completely eroded (Fig. 7). In general, we conclude that breakthrough faults can develop anywhere in the forelimb of the hanging wall block (cf. Mitra and Mount, 1998, p. 74).

6. Estimation of long-term displacement

Total lithospheric shortening associated with the Whittier fault has been estimated by restoring the Soquel Member to its predeformation bed length on six cross-sections, A through F (Fig. 11), distributed evenly along the Whittier fault and parallel to the N–S direction of tectonic transport. Together these sections represent our historical or 4-D analysis of the Whittier structure. From this analysis, we conclude that horizontal contraction increases from southeast to northwest along the Whittier fault from 1.4 km at the Esperanza oil field to 3.2 km near the Whittier Narrows (Fig. 11). The greater shortening at Whittier Narrows may reflect interaction between the Whittier fault, and either the Whittier Narrows earthquake fault or structures associated with the Elysian Park anticline (Fig. 1), all of which meet near the Whittier Narrows. Alternatively, contraction may have begun earlier in the Whittier Narrows and progressed southeastward.

Shortening estimates are most reliable for the central segment of the Whittier fault, where the structure of the

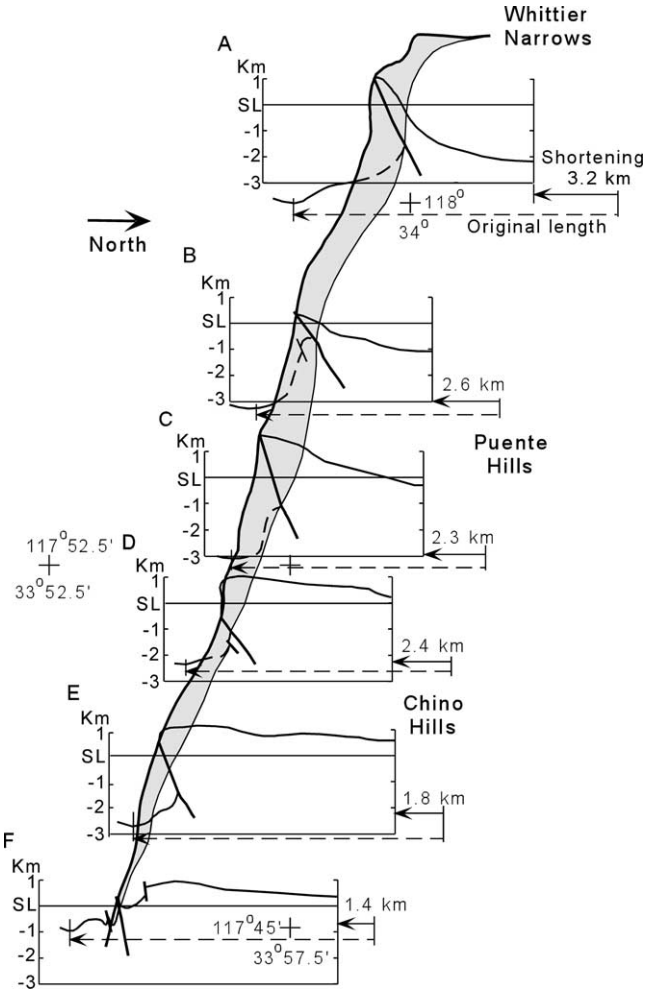

Fig. 11. N–S profiles A through F across the Whittier fault showing shortening at the top of the Soquel Member. View of the profiles is from east to west. The E–W dimension has been slightly exaggerated so that the cross-sections do not overlap. The latitude and longitude intersections are located at sea level. The shaded area is a generalized representation of the Whittier fault to approximate a 3-D perspective between the sections. The amount of horizontal contraction (solid arrow) is the difference between the original bed length of the top of the Soquel between two points on each section (dashed arrow) and the present horizontal distance between the same two points. Profile D is near cross-section A–A′ (Fig. 6).

hanging wall block is relatively simple, and the architecture of the Soquel Member is reasonably constrained by well data and outcrops. The average horizontal contraction for four, N–S profiles across the central segment is 2.3 km (Fig. 11). Accordingly, the average rate of horizontal contraction over the past 8 My is estimated at 0.3 mm/year. Assuming fault breakthrough at ca. 1.0 Ma, the rate of horizontal contraction since fault breakthrough during the past million years may have been faster, perhaps as fast as 1.0 mm/year (Fig. 10c). The components of the total N–S average horizontal displacement of 2.3 km, parallel and perpendicular to the N70W strike of the central part of the Whittier fault, are 2.2 and 0.8 km, respectively, yielding a ratio of strike-slip to dip-slip displacement of about 0.4.

Uncertainties associated with shortening estimates are difficult to quantify. The tectonic transport direction is geometrically constrained by earthquake mechanisms along the northwestern segment, but could be in a different direction along the southeastern segment. Projections of the top of the Soquel sandstone above the ground level in areas of steep dip on the hanging wall block could have introduced errors in bed-length estimates. Likewise, in areas with few deep wells along the footwall block, estimates of the top of the Soquel Member are based on the projection of stratigraphic thicknesses from shallow wells and are subject to error. If secondary faults that have not been recognized offset the Soquel Member, then the amount of shortening would be overestimated. If our estimated tectonic transport direction were in error, our assumption of plane-strain would not be valid. In such a case, our shortening estimates would be maxima, and the cross-sections could not be balanced accurately with two-dimensional analyses. However, an error of 30° azimuth in the transport direction would only produce about a 15% error in estimates of shortening. Qualitatively, we estimate that our estimate of average horizontal contraction for the past ca. 8 My is in error by less than 50%.

7. Conclusions

The availability of data from hundreds of wells, several vintages of surface geologic maps and focal-mechanism solutions from the 1987 Whittier Narrows earthquake and its aftershocks have allowed us to make a 4-D structural interpretation of the evolution of the Whittier fold–fault system. Integration of that interpretation with stratigraphic information from wells and outcrops has led to the following three-phase model.

1. Formation of a half-graben accompanied by volcanic activity and by deposition of marine, siliciclastic sedimentary strata north of the proto-Whittier normal fault, which occupied approximately the present position of the Whittier fault between ca. 14 and ca. 8 Ma.
2. Inversion of the half-graben and uplift of the Puente Hills anticline above a Whittier blind reverse fault between ca. 8 and ca. 1 Ma. The center of deposition shifted during the uplift from the graben to a narrow trough south of the rising Puente Hills.
3. Breakthrough of the through-going Whittier reverse fault onto the seafloor at ca. 1 Ma.

Based on slip vectors from the Whittier Narrows earthquakes and the geometric constraints of 3-D structural interpretation, we have concluded that the tectonic transport direction of the Whittier fault has been N–S for the past ca. 8 My. Total shortening for that time interval ranges from ca. 3.2 km near the Whittier Narrows to ca. 1.4 km near Santa Ana Canyon and averages 2.3 km over the length of

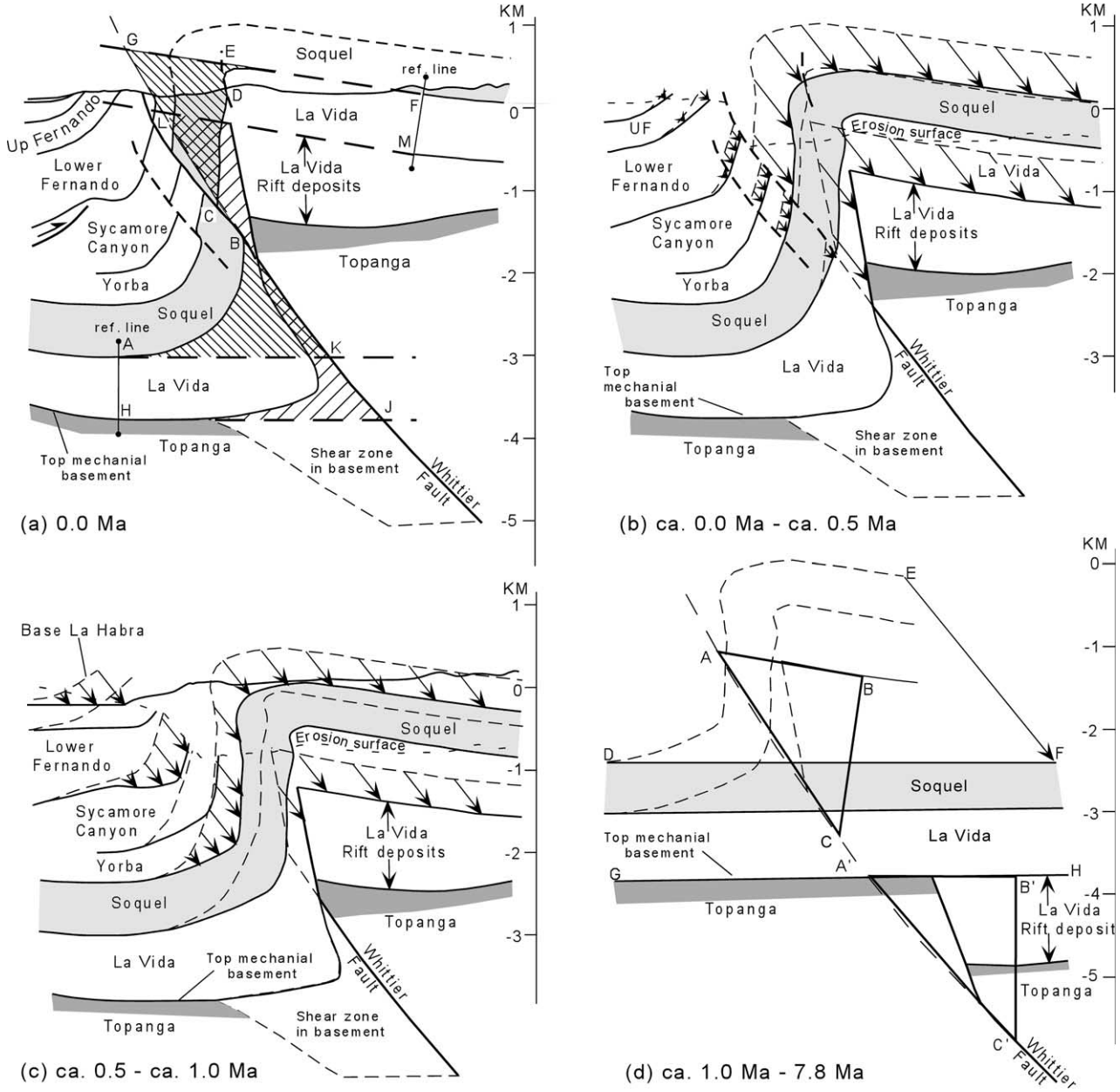

the Whittier fault. The average rate of shortening has therefore been 0.3 mm/year, although the rate since surface breakthrough at ca. 1 Ma may be as high as 1.0 mm/year. The ratio of strike-slip to dip-slip displacement on the Whittier fault is about 0.4.

Acknowledgements

Data used in this study and field access have been generously provided by Aera Energy LLC (formerly Shell Oil Company), Nuevo Energy Company, Unocal, Oregon State University, United States Geological Survey, Earth Consultants International, SunCal Companies, California Division of Mines and Geology, California Division of Oil, Gas & Thermal Resources, California Department of Parks and Recreation and the Harvest Development Company.

We have benefited from discussions with Gary Beckerman, Siang Tan, Eldon Gath, Kay St. Peters, Tania Gonzalez, Russell Miller, David Herzog, Gary Huftile, Tom Rockwell, Robert S. Miller, Peter Rumelhart and Andrew Meigs. Our manuscript benefited from editing by Jim Evans, Jonathon Nourse, Mark P. Fischer, R.V. Ingersoll, L.A. Beyer and Mike Oskin. The senior author thanks the members of his Ph.D. dissertation committee, Kevin Burke, John F. Casey, Robert S. Yeats and Hua-Wei Zhou. We especially acknowledge that this study could not have been completed without Bob Yeats' experience and knowledge of Los Angeles basin geology and its structural evolution and his patient readiness to share his knowledge and thoughts with us.

Appendix A. Structural model for balancing and restoring cross-sections

We have modeled the Whittier fault and the Puente Hills anticline as basement-involved structures (cf. Erslev, 1986; Cook, 1988; Williams et al., 1989; Mitra, 1993; Narr and Suppe, 1994). In the model, these structures have developed by inversion of a half-graben along a basement-involved reverse fault, producing the nearly vertical forelimb and the gently north-dipping back-limb that characterize the central segment of the Whittier fault system. Five assumptions of the model constrain our interpretation of the cross-sections of the central segment of the Whittier fault.

1. In crystalline basement, the Whittier fault can be represented by a single master fault, and the total horizontal contraction of the Soquel Member is equal to the heave at the master fault.
2. Because deformation of the Soquel Member is predominantly by flexural-slip, bed length has been conserved during deformation and can be directly determined from cross-sections through the deformed strata.
3. The predeformation lengths of the Soquel Member and the top of the mechanical basement are the same.
4. No significant relative movement between the basement and the sedimentary cover has occurred at the axis of the La Habra syncline or in the hanging wall block of the Whittier fault.
5. Deformation along the cross-section can be described by plane strain.

The top of mechanical basement has been taken to be the Topanga sandstone south of the Whittier fault and the top of the lower La Vida siltstone, diabase sill and sandstone rift-fill north of the fault, because of the contrast in competence between the La Vida siltstone and the underlying units. Mechanical basement on both sides of the Whittier fault consists mainly of well-cemented sedimentary strata and igneous and metamorphic rocks. The La Vida siltstone overlying mechanical basement is thinly bedded and commonly intensely sheared and folded in outcrop (cf. Durham and Yerkes, 1964, p. B13). We consider that the sedimentary strata above the La Vida siltstone deformed by flexural slip and some faulting. Mechanical basement deformed dominantly by brittle failure. The intervening La Vida siltstone passively folded to accommodate the shape of the space developed between the overlying and underlying units (cf. Cook, 1988). A triangular-shaped zone in the footwall basement block probably developed by some combination of simple shear, brecciation, cataclastic flow and rigid body translation and rotation (Cook, 1988; Evans et al., 1993; Narr and Suppe, 1994). Because of the lack of field and well data, such zones are represented in our cross-sections only as generalized deformation zones. The existence of such a footwall deformation zone is suggested by outcrops east of Esperanza oil field that exhibit steeply dipping to overturned beds and numerous faults overlain in places by chaotic deposits of colluvium and alluvium and landslide blocks (Durham and Yerkes, 1964; Hannan et al., 1979; Tan et al., 1984). A deformation zone in the basement rocks is required to balance the cross-sections. The application of the model and restoration technique to cross-section A–A′ (Fig. 6) are illustrated in Fig. 12.

References

Atwater, T., 1970. Implications of plate tectonics for the Cenozoic tectonic evolution of western North America. Geological Society of America Bulletin 81 (12), 3513–3535.

Axen, G.J., 2000. New palinspastic reconstructions of the southern San Andreas fault system and northern Gulf of California at 2, 4, 6.5, and 12 Ma. Eos Trans. AGU 81 (48), F1243.

Fig. 12. Methods used to balance and retrodeform cross-section A–A′ (Fig. 6). (a) Area and bed length relationships that result in a balanced cross-section at 0.0 Ma and constrain the dip of the master basement fault. No significant motion of the cover relative to the basement takes place at the reference lines (barbell symbols). Between the reference lines, the bed length of the base of the Soquel Member is assumed to be unchanged during deformation and to equal the bed length of the top of the mechanical basement before deformation. The heavy dashed lines projected from the reference lines in the footwall and hanging wall blocks at the top of basement and at the base of the Soquel Member are construction aids (cf. Cook, 1988). The master basement fault and its projection into the cover units have been drawn such that (1) line segments AK + GF and HJ + LM are both equal in length to the bed length of the base of the Soquel (AB + CD + EF) and (2) the cross-sectional areas of rock units before and after deformation are equal. To satisfy the latter requirement, the area of basement above the projected basement top in the footwall block equals the area of basement below the projected top in the hanging wall block (triangles with left-diagonal lines), and the area of La Vida siltstone above the projected base of Soquel in the footwall block equals the area of La Vida below the projected top in the hanging wall block (triangles with right-diagonal lines) (cf. Cook, 1988). (b) Restoration from 0.0 to ca. 0.5 Ma by removal of fault displacements in Upper Miocene and Pliocene strata. Restoration vectors (arrows) are approximately parallel to the dip of the basement fault and equal in magnitude to total fault displacements (cf. Novoa et al., 2000). Because of the shortness of the displacements, the effect of rotation of the hanging wall basement block along the curved basement fault has not been included in the analysis. (c) Restoration from ca. 0.5 to ca. 1.0 Ma by rotation of the base of the La Habra Formation to horizontal. Restoration vectors (arrows) are approximately parallel to the dip of the basement fault. The magnitudes of the vectors are defined by the distances between the base of the La Habra and the horizontal (upper left arrows in diagram). A constant displacement equal to the maximum displacement of the base of the La Habra at its outcrop has been applied to the upper forelimb and backlimb strata where the La Habra has been eroded. That displacement is a minimum value for the hanging wall block and implies that eroded La Habra strata occupied the backlimb of the fold, i.e. prior to erosion, the anticlinal hinge line at the base of the La Habra Formation was in the vicinity of the updip limit of the La Habra outcrop. The actual location of the La Habra hinge line is indeterminate. The topographic profile is conceptual to illustrate a likely source area for the clasts of the Puente Formation found in the Pleistocene strata (Yerkes, 1972). (d) Restoration from ca. 1.0 to ca. 7.8 Ma by rotation of the hanging wall block to horizontal. Triangle ABC is restored to A′B′C′ along the curvature of the fault, and line segment DE (top of the Soquel Member) is restored to line segment DF. Line segments DE, DF and GH are equal in length, and cross-sectional areas balance.

Banks, P.O., Silver, L.T., 1966. Evaluation of the decay constant of uranium-238 from lead isotope ratios. Journal of Geophysical Research 71 (16), 4037–4046.

Barron, J.A., Isaacs, C.M., 2001. Updated chronostratigraphic framework for the California Miocene. In: Isaacs, C.M., Rullkotter, J. (Eds.). The Monterey Formation: From Rocks to Molecules. Columbia University, New York, pp. 393–395.

Barth, A.P., Schneiderman, J.S., 1996. A comparison of structures in the Andean Orogen of northern Chile and exhumed midcrustal structures in Southern California, USA: an analogy in tectonic style? International Geology Review 38 (12), 1075–1085.

Berggren, W.A., Kent, D.V., Swisher, C.C., Aubry, M.-P., 1995. A Revised Cenozoic Geochronology and Chronostratigraphy. In: Berggren, W.A., Kent, D.V., Aubry, M.-P, Hardenbol, J. (Eds.), Geochronology Time Scales and Global Stratigraphic Correlations. Society of Economic Paleontologists and Mineralogists Special Publication 54, pp. 129–212.

Blake, G.H., 1991. Review of the Neogene biostratigraphy and stratigraphy of the Los Angeles basin and implications for basin evolution. In: Biddle, K.T. (Ed.), Active Margin Basins. American Association of Petroleum Geologists Memoir 52, pp. 135–184.

Brown, W.G., 1988. Deformational style of Laramide uplifts in the Wyoming foreland. In: Schmidt, C.J., Perry, W.J. (Eds.), Geological Society of America Memoir 171, pp. 1–25.

Bullard, T.F., Lettis, W.R., 1993. Interaction of the Rocky Mountain foreland and the Cordilleran thrust belt. Quaternary fold deformation associated with blind thrust faulting, Los Angeles basin, California. In: Stout, M.L. (Ed.). Proceedings of the 35th Annual Meeting of the Association of Engineering Geologists, pp. 659–678.

Cook, D.G., 1988. Balancing basement-cored folds of the Rocky Mountain foreland. In: Schmidt, C.J., Perry, W.J., Jr. (Eds.), Interaction of the Rocky Mountain Foreland and the Cordilleran Thrust Belt. Geological Society of America Memoir 171, pp. 53–64.

Crouch, J.K., Suppe, J., 1993. Late Cenozoic tectonic evolution of the Los Angeles basin and inner California borderland: a model for core complex-like crustal extension. Geological Society of America Bulletin 105 (11), 1415–1434.

Daviess, S.N., Woodford, A.O., 1949. Geology of the northwestern Puente Hills, Los Angeles County, California. U.S. Geological Survey Oil and Gas Investigations Preliminary Map 83.

Davis, T.L., Namson, J., Yerkes, R.F., 1989. A cross-section of the Los Angeles area: seismically active fold and thrust belt, the 1987 Whittier Narrows earthquake, and earthquake hazard. Journal of Geophysical Research 94 (B7), 9644–9664.

Dickinson, W.R., Lawton, T.F., 2001. Carboniferous to Cretaceous assembly and fragmentation of Mexico. Geological Society of America Bulletin 113(9), 1142–1160.

Durham, D.L., Yerkes, R.F., 1964. Geology and oil resources of the eastern Puente Hills area, southern California. U.S. Geological Survey Professional Paper 420-B.

English, W.A., 1926. Geology and oil resources of the Puente Hills region, southern California. U.S. Geological Survey Bulletin 768.

Erslev, E.A., 1986. Basement balancing of Rocky Mountain foreland uplifts. Geology 14 (3), 259–262.

Evans, J.P., Dubois, M.A., Batatian, D., Derr, D.N., Harlan, S.S., Malizzi, L., McDowell, R.J., Nelson, G.C., Parke, M., Schmidt, C.J., Weberg, E.D., 1993. Deformation mechanisms and kinematics of a Precambrian-cored fold and fault structure. In: Schmidt, C.J., Chase, R.B., Erslev, E.A. (Eds.), Laramide Basement Deformation in the Rocky Mountain Foreland of the Western United States. Geological Society of America Special Paper 280, pp. 163–176.

Fife, D.L., Minch, J.A., Crampton, P.J., 1967. Late Jurassic age of the Santiago Peak Volcanics, California. Geological Society of America Bulletin 78 (2), 299–303.

Gath, E.M., Gonzalez, T., Rockwell, T.K., 1992. Evaluation of the Late Quaternary rate of slip, Whittier fault, Southern California. U.S. Geological Survey Final Technical Report—Contract No. 14-08-0001-G1696.

Gath, E.M., Gonzalez, T., Drumm, P.L., Buchiarelli, P., 1994. A paleoseismic investigation at the northern terminus of the Whittier fault zone, in the Whittier Narrows area, Rosemead, California. Southern California Earthquake Center Final Technical Report, Draft Version 5/18/94.

Gourley, J.W., 1975. Upper Miocene Puente Formation in the Whittier Hills and surrounding region. In: Truex, J.N. (Ed.), A Tour of the Oil Fields of the Whittier Fault Zone, Los Angeles Basin, California. Pacific Sections, American Association of Petroleum Geologists–Society of Exploration Geophysicists–Society of Exploration Paleontologists and Mineralogists, Joint Annual Field Trip, April 26 1975, pp. 13–24.

Gray, C.H., Jr., 1961. Geology of the Corona South quadrangle and the Santa Ana Narrows area, Riverside, Orange, and San Bernardino counties, California and Mines and Mineral Deposits of the Corona South quadrangle, Riverside, Orange, and San Bernardino counties, California. California Division of Mines Bulletin 178.

Greenwood, R., Morton, D.M., 1991. Geologic map of the Santa Ana 1:100,000 scale quadrangle, California. Department of Conservation, Division of Mines and Geology Open-File Report 91-17.

Hannan, D.L., Lung, R., Leighton, F.B., 1979. Geologic investigation of recency of fault activity by surface trenching on the Whittier fault, California. Final Technical Report, U.S. Geological Survey Contract No. 14-08-0001-16821, Leighton and Associates.

Harding, T.P., 1990. Identification of wrench faults using subsurface structural data: criteria and pitfalls. American Association of Petroleum Geologists Bulletin 74 (10), 1590–1609.

Hauksson, E., Jones, L.M., 1989. The 1987 Whittier Narrows earthquake sequence in Los Angeles, Southern California: seismological and tectonic analysis. In: Anonymous (Ed.), Special Section on Whittier Narrows Earthquake. Journal of Geophysical Research, B, Solid Earth and Planets 94, pp. 9569–9589.

Heath, E.G., 1954. Geology along the Whittier Fault north of Horseshoe Bend, Santa Ana Canyon, California. Master's thesis, Claremont Graduate School (Pomona College).

Herzog, D.W., 1998. Subsurface structural evolution along the northern Whittier fault zone of the eastern Los Angeles basin, Southern California. Master's thesis, Oregon State University.

Hill, M.L., 1954. Tectonics of faulting in southern California. In: Jahns, R.H. (Ed.), Geology of Southern California. California Division of Mines Bulletin 170 (4), pp. 5–14.

Hornafius, J.S., Luyendyk, B.P., Terres, R.R., Kamerling, M.J., 1986. Timing and extent of Neogene tectonic rotation in the western Transverse Ranges, California. Geological Society of America Bulletin 97, 1476–1487.

Hull, A.G., Nicholson, C., 1992. Seismotectonics of the northern Elsinore fault zone, Southern California. Bulletin of the Seismological Society of America 82 (2), 800–818.

Imlay, R.W., 1964. Middle and Upper Jurassic fossils from southern California. Journal of Paleontology 38, 505–509.

Ingersoll, R.V., Rumelhart, P.E., 1999. Three-stage evolution of the Los Angeles basin, Southern California. Geology 27 (7), 593–596.

Lamar, D.L., 1961. Structural evolution of the northern margin of the Los Angeles basin. Ph.D. thesis, University of California, Los Angeles.

Lang, H.R., 1978. Late Cretaceous biostratigraphy of the southeastern Los Angeles basin. California Division of Oil and Gas Report No. TR20.

Larsen Jr, E.S., Gottfried, D., Jaffee, H.W., Waring, C.L., 1958. Lead-alpha ages of the Mesozoic batholiths of North America. U.S. Geological Survey Bulletin 1070-B, 35–62.

Luyendyk, B.P., 1991. A model for Neogene crustal rotations, transtension, and transpression in southern California. Geological Society of America Bulletin 103, 1528–1536.

Mayer, L., 1991. Central Los Angeles basin: Subsidence and thermal implications for tectonic evolution. In: Biddle, K.T. (Ed.). Active Margin Basins. American Association of Petroleum Geologists Memoir 52, pp. 185–195.

McCulloh, T.H., Beyer, L.A., Enrico, R.J., 2000. Paleogene strata of the

eastern Los Angeles basin, California: paleogeography and constraints on Neogene structural evolution. Geological Society of America Bulletin 112 (7), 1155–1178.

Mitra, S., 1993. Geometry and kinematic evolution of inversion structures. American Association of Petroleum Geologists Bulletin 77 (7), 1159–1191.

Mitra, S., Mount, V.S., 1998. Foreland basement-involved structures. American Association of Petroleum Geologist Bulletin 82 (1), 70–109.

Morton, J.L., Morton, D.M., 1979. K–Ar ages of Cenozoic volcanic rocks along the Elsinore fault zone, southwestern Riverside County, California. Geological Society of America Abstracts with Programs (11), 119.

Narr, W., Suppe, J., 1994. Kinematics of basement-involved compressive structures. American Journal of Science 294 (7), 802–860.

Nicholson, C., Sorlien, C.C., Atwater, T., Crowell, J.C., Luyendyk, B.P., 1994. Microplate capture, rotation of the western Transverse Ranges, and initiation of the San Andreas transform as a low-angle fault system. Geology 22 (6), 491–495.

Nilsen, T.H., 1987. Paleogene tectonics and sedimentation of coastal California. In: Ingersoll, R.V., Ernst, W.G. (Eds.). Cenozoic Basin Development of Coastal California, pp. 81–123.

Nourse, J.A., Weigand, P.W., Hazelton, G.B., 1998. Igneous and tectonic response of the eastern San Gabriel Mountains to Neogene extension and rotation of the Transverse Ranges block. In: Behl, R.J. (Ed.), Guidebook to Field Trip no. 10: Long Beach, California, California State University, Cordilleran Section, Geological Society of America, pp. 10-1–10-15.

Novoa, E., Suppe, J., Shaw, J.H., 2000. Inclined-shear restoration of growth folds. American Association of Petroleum Geologists Bulletin 84 (6), 787–804.

Oskin, M., Stock, J., Martin-Batajas, A., Lewis, C., 2000. Rapid localization of Pacific–North American plate motion in the Gulf of California. Geology 29 (5), 459–462.

Redin, T., 1991. Oil and gas production from submarine fans of the Los Angeles basin: a guide to migration history. In: Biddle, K.T. (Ed.), Active Margin Basins. American Association of Petroleum Geologists Memoir 52, pp. 239–259.

Rumelhart, P.E., Ingersoll, R.V., 1997. Provenance of the upper Miocene Modelo Formation and subsidence analysis of the Los Angeles basin, Southern California: implications for paleotectonic and paleogeographic reconstructions. Geological Society of America Bulletin 109 (7), 885–899.

Sage, O.G., Jr., 1975. Paleocene geography of the Los Angeles region. In: Weaver, D.W., Hornaday, G.R., Tipton, A. (Eds.), Conference on Future Energy Horizons of the Pacific Coast, Paleogene Symposium and Selected Technical Papers. Pacific Sections, American Association of Petroleum Geologists–Society of Exploration Paleontologists and Mineralogists–Society of Exploration Geophysicists, Annual Meetings, pp. 417–438.

Schoellhamer, J.E., Vedder, J.G., Yerkes, R.F., Kinney, D.M., 1981. Geology of the northern Santa Ana Mountains, California. U.S. Geological Survey Professional Paper 420-D.

Tan, S.S., Miller, R.V., Evans, J.R., 1984. Environmental geology of parts of the La Habra, Yorba Linda and Prado Dam quadrangles, Orange County, California. California Division of Mines and Geology Open-File Report 84-24.

Turner, D.L., 1970. Potassium–argon dating of Pacific Coast Miocene foraminiferal stages. Geological Society of America Special Paper 124, 91–129.

West, J.C., Redin, T.W., 1990. Correlation section across northern Los Angeles basin from Santa Monica bay to Prado flood control basin. Pacific Section, American Association of Petroleum Geologists CS 28.

West, J.C., Redin, T.W., 1991. Correlation section across eastern Los Angeles basin from San Pedro Bay to San Gabriel Mountains. Pacific Section American Association of Petroleum Geologists CS 3R.

Williams, G.D., Powell, C.M., Cooper, M.A., 1989. Geometry and kinematics of inversion tectonics. In: Cooper, M.A, Williams, G.D. (Eds.), Inversion Tectonics, Geological Society Special Publications 44, pp. 3–15.

Wissler, S.G., 1943. Stratigraphic Formations of the producing zones of the Los Angeles basin oil fields. Division of Mines and Geology Bulletin 118, 209–234.

Wolf, R.A., Farley, K.A., Silver, L.T., 1997. Assessment of (U–Th)/He thermochronometry: the low-temperature history of the San Jacinto Mountains, California. Geology 25 (1), 65–68.

Woodford, A.O., Shelton, J.S., Moran, T.G., 1944. Geology and oil possibilities of Puente and San Jose hills, California. U.S. Geological Survey Oil and Gas Investigations Preliminary Map 23.

Woodford, A.O., Schoellhamer, J.E., Vedder, J.G., Yerkes, R.F., 1954. Geology of the Los Angeles basin. In: Jahns, R.H. (Ed.), Geology of Southern California. California Division of Mines Bulletin 170 (2), pp. 65–81.

Wright, T.L., 1991. Structural geology and tectonic evolution of the Los Angeles basin, California. In: Biddle, K.T. (Ed.), Active Margin Basins. American Association of Petroleum Geologists Memoir 52, pp. 35–134.

Yeats, R.S., Beall, J.M., 1991. Stratigraphic controls of oil fields in the Los Angeles basin: a guide to migration history. In: Biddle, K.T. (Ed.), Active Margin Basins. American Association of Petroleum Geologists Memoir 52, pp. 221–237.

Yeats, R.S., Huftile, G.J., 1997. Tectonics of the Montebello anticline, the East Montebello fault, and the 1987 Whittier Narrows earthquake. In: Aki, K. (Ed.), The 1996 Southern California Earthquake Center (SCEC) Annual Report. Progress reports from SCEC scientists II, pp. C.75–C.79.

Yerkes, R.F., 1972. Geology and oil resources of the western Puente Hills area, Southern California. U.S. Geological Survey Professional Paper 420-C.